The Drosophila Baramicin polypeptide gene protects against fungal infection

M.A. Hanson[1*], L.B. Cohen[2], A. Marra[1], I. Iatsenko[1,3], S.A. Wasserman[2], and B. Lemaitre[1]

1 Global Health Institute, School of Life Science, École Polytechnique Fédérale de Lausanne (EPFL), Lausanne, Switzerland.
2 Division of Biological Sciences, University of California San Diego (UCSD), La Jolla, California, United States of America.
3 Max Planck Institute for Infection Biology, 10117, Berlin, Germany.
* Corresponding author: M.A. Hanson (mark.hanson@epfl.ch), B. Lemaitre (bruno.lemaitre@epfl.ch)

ORCID IDs:
Hanson: https://orcid.org/0000-0002-6125-3672
Cohen: https://orcid.org/0000-0002-6366-570X
Iatsenko: https://orcid.org/0000-0002-9249-8998
Wasserman: https://orcid.org/0000-0003-1680-3011
Lemaitre: https://orcid.org/0000-0001-7970-1667

Abstract (212 words)

The fruit fly *Drososphila melanogaster* combats microbial infection by producing a battery of effector peptides that are secreted into the haemolymph. The existence of many effectors that redundantly contribute to host defense has hampered their functional characterization. As a consequence, the logic underlying the role of immune effectors is only poorly defined, and exactly how each gene contributes to survival is not well characterized. Here we describe a novel *Drosophila* antifungal peptide gene that we name *Baramicin A*. We show that *BaraA* encodes a precursor protein cleaved into multiple peptides via furin cleavage sites. *BaraA* is strongly immune-induced in the fat body downstream of the Toll pathway, but also exhibits expression in the nervous system. Importantly, we show that flies lacking *BaraA* are viable but susceptible to a subset of filamentous fungi. Consistent with *BaraA* being directly antimicrobial, overexpression of *BaraA* promotes resistance to fungi and the IM10-like peptides produced by *BaraA* synergistically

inhibit growth of fungi in vitro when combined with a membrane-disrupting antifungal. Surprisingly, *BaraA* males but not females display an erect wing phenotype upon infection, pointing to an adaptive role for *BaraA* on the wing muscle or the nervous system. Collectively, we identify a new antifungal immune effector downstream of Toll signalling, improving our knowledge of the *Drosophila* antimicrobial response.

Significance statement

Antimicrobial peptides (AMPs) of the innate immune system provide a front line of defence against infection. Recently AMPs have been implicated in physiological processes including inflammation, aging, and neurodegeneration. *Drosophila melanogaster* has been a useful model for understanding AMP functions and specificities in vivo. Here we describe a new *Drosophila* AMP family, *Baramicin*, which protects flies against fungal infection. The *Baramicin* polypeptide structure is also unique amongst animal AMPs, encoding multiple peptides on a single protein precursor cleaved by furin. Furthermore *Baramicin* mutants display a behavioural response to infection, suggesting Baramicin AMPs interact with more than just pathogens. *Baramicin* adds to our knowledge of the potent *Drosophila* antifungal response, and to growing observations of AMPs acting in seemingly non-canonical roles.

Introduction (806 words)

The innate immune response provides the first line of defence against pathogenic infection. This reaction is usually divided into three stages: i) the recognition of pathogens through dedicated pattern recognition receptors, ii) the activation of conserved immune signalling pathways and iii) the production of immune effectors that target invading pathogens [1,2]. The study of invertebrate immune systems has led to key observations of broad relevance, such as the discovery of phagocytosis [3], antimicrobial peptides (AMPs) [4], and the implication of Toll receptors in metazoan immunity[5]. Elucidating immune mechanisms, genes, and signalling pathways has greatly benefited from investigations in the fruit fly *Drosophila melanogaster*, which boasts a large suite of molecular and genetic tools for manipulating the system. One of the best-characterized immune reactions of *Drosophila* is the systemic immune response.

This reaction involves the fat body (an analog of the mammalian liver) producing immune effectors that are secreted into the haemolymph. In *Drosophila*, two NF-κB signalling pathways, the Toll and Imd pathways, regulate most inducible immune effectors: the Toll pathway is predominantly activated in response to infection by Gram-positive bacteria and fungi [5,6], while the immune-deficiency pathway (Imd) responds to the DAP-type peptidoglycan most commonly found in Gram-negative bacteria and a subset of Gram-positive bacteria [7]. These two signalling pathways regulate a transcriptional program that results in the massive synthesis and secretion of humoral effector peptides [6,8]. Accordingly, mutations affecting the Toll and Imd pathways cause extreme susceptibilities to systemic infection that reflect the important contribution of these pathways to host defence. The best-characterized immune effectors downstream of these pathways are antimicrobial peptides (AMPs). AMPS are small and often cationic peptides that disrupt the membranes of microbes, although some have more specific mechanisms [9]. Multiple AMP genes belonging to seven well-characterized families are induced upon systemic infection [10]. However transcriptomic analyses have revealed that the systemic immune response encompasses far more than just the canonical AMPs. Many uncharacterized genes encoding small secreted peptides are induced to high levels downstream of the Toll and Imd pathways, pointing to the role for these peptides as immune effectors [11]. In parallel, MALDI-TOF analyses of the haemolymph of infected flies revealed the induction of 24 peaks - mostly corresponding to uncharacterized peptides - that were named “IMs” for Immune-induced Molecules (IM1-IM24) [8]. Many of the genes that encode these components of the immune peptidic secretome have remained largely unexplored. This is mainly due to the fact that these IMs belong to large gene families of small-sized genes that were until recently difficult to disrupt by mutagenesis.

The CRISPR/Cas9 gene editing approach now allows the necessary precision to delete small genes, singly or in groups, providing the opportunity to dissect effector peptide functions. In 2015 a family of 12 related IM-encoding genes, unified under the name *Bomanins*, were shown to function downstream of Toll. Importantly,

a deletion removing 10 out of the 12 Bomanins revealed their potent contribution to defence against both Gram-positive bacteria and fungi [12]. While Bomanins contribute significantly to Toll-mediated defence, their molecular functions are still unknown and it is unclear if they are directly antimicrobial [13]. Two other IMs encoding IM4 and IM14 (renamed *Daisho1* and *Daisho2*, respectively) were shown to contribute downstream of Toll to resistance against specific fungi. Interestingly, Daisho peptides bind to fungal hyphae, suggesting direct antifungal activity [14]. Finally a systematic knock-out analysis of *Drosophila* AMPs revealed that they play an important role in defence against Gram-negative bacteria and some fungi, but surprisingly little against Gram-positive bacteria [15]. An unforeseen finding from these recent studies is the high degree of AMP-pathogen specificity: this is perhaps best illustrated by the specific requirement for *Diptericin*, but not other AMPs, in defence against *Providencia rettgeri* [15,16]. Collectively, these studies in *Drosophila* reveal that immune effectors can be broad or specific in mediating host-pathogen interactions. Understanding the logic of the *Drosophila* effector response will thus require a careful dissection of the remaining uncharacterized IMs.

Previous studies identified an uncharacterized Toll-regulated gene called *IMPPP/CG33470*, which we rename "*BaraA*" (see below), that encodes several IMs, indicating a role in the humoral response. Here, we have improved the annotation of IMs produced by *BaraA* to include: IM10, IM12 (and its sub-peptide IM6), IM13 (and its sub-peptides IM5 and IM8), IM22, and IM24. Using a *BaraA* reporter, we show that *BaraA* is not only immune-induced in the fat body, but also highly expressed in the nervous system. Importantly, we show that flies lacking *BaraA* are viable but susceptible to specific infections, notably by the entomopathogenic fungus *Beauveria bassiana*. Consistent with this, the IM10-like peptides produced by *BaraA* inhibit fungal growth in vitro when combined with the antifungal Pimaricin. Surprisingly, *BaraA* deficient males also display a striking erect wing behaviour upon infection. Collectively, we identify a new antifungal immune effector downstream of Toll signalling, improving our knowledge of the *Drosophila* antimicrobial response.

Results (2923 words):

BaraA is regulated by the Toll pathway

Previous microarray studies from De Gregorio et al. [11] suggest that *BaraA* is primarily regulated by the Toll pathway, with a minor input from the Imd pathway (**Fig.** 1A and **Fig.** S1A-F). Consistent with this, we found several putative NF-κB binding sites upstream of the *BaraA* gene (guided by previous reports [17–19]). Notably there are two putative binding sites for Relish, the transcription factor of the Imd pathway and three putative binding sites for the Dif/Dorsal transcription factors acting downstream of Toll (**Fig.** S1G). We challenged wild-type flies and Imd or Toll pathway mutants (Rel^{E20} and spz^{rm7} respectively) with the Gram-negative bacterium *Escherichia coli*, the yeast *Candida albicans*, or the Gram-positive bacterium *Micrococcus luteus*. RT-qPCR analysis confirms that *BaraA* is induced by infection with *E. coli*, *C. albicans*, or *M. luteus (***Fig.** 1B and **Fig.** S1H). *BaraA* remains highly inducible in a *Relish* mutant background, albeit at slightly reduced level compared to the wild-type. However *BaraA* expression is abolished in spz^{rm7} flies. Collectively, the expression pattern of *BaraA* is reminiscent of the antifungal peptide gene *Drosomycin* with a primary input by the Toll pathway and a minor input from the Imd pathway [10,20].

To further characterize the expression of *BaraA*, we generated a *BaraA-Gal4* transgene in which 1675bp of the *BaraA* promoter sequence is fused to the yeast transcription factor Gal4. Use of *BaraA-Gal4>UAS-mCD8-GFP* (referred to as *BaraA>mGFP*) reveals that *BaraA* is strongly induced in the fat body 60h post infection by *M. luteus* (**Fig.** 1C), but less so by *E. coli* pricking (**Fig.** S1I); dissections confirmed this GFP signal is produced by the fat body. Larvae pricked with *M. luteus* also show a robust GFP signal primarily stemming from the fat body when examined 2hpi (**Fig.** 1D). We also observed a strong constitutive GFP signal in the headcase of

164 adults (**Fig.** 1E), including the border of the eyes and the ocelli (**Fig.** 1F). Dissection
165 confirmed that the *BaraA* reporter is expressed in brain tissue, notably in the central
166 ventral brain furrow. Other consistent signals include GFP in the wing veins and
167 subcutaneously along borders of thoracic pleura in adults (**Fig.** 1G-H), and in
168 spermatheca of females (**Fig.** S1J). There was also sporadic GFP signal in other
169 tissues that included the larval hindgut, the dorsal abdomen of developing pupae,
170 and the seminal vesicle of males.

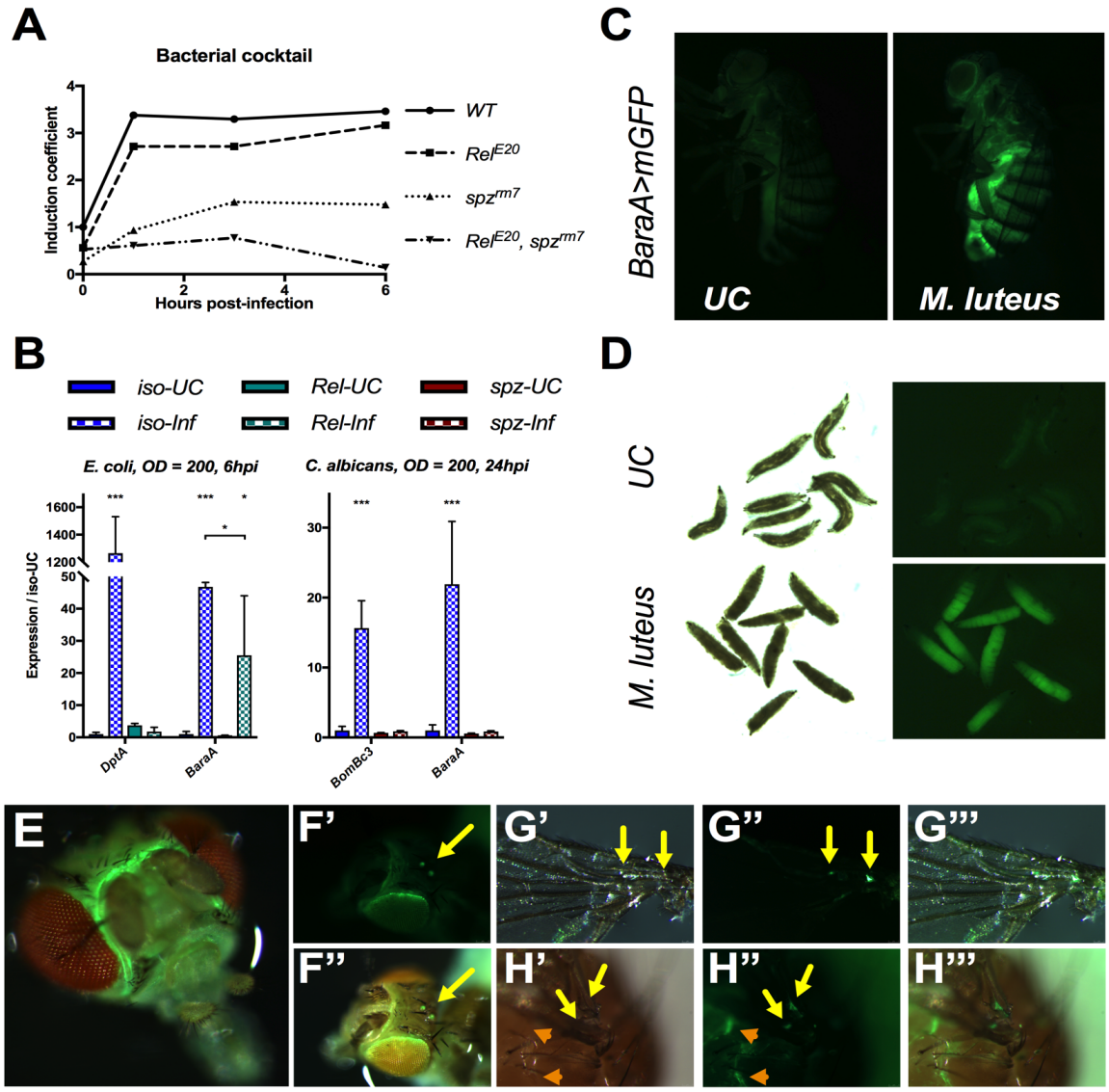

Figure 1: *BaraA* is an immune-induced gene regulated by the Toll pathway. **A)** Expression profile of *BaraA* upon bacterial challenge by a mix of *E. coli* and *M. luteus* (values from De Gregorio *et al.* [1]). *spz*^{rm7} flies lacking Toll signalling have severely reduced *BaraA* expression, and *BaraA* induction is totally abolished in *Rel*^{E20}, *spz*^{rm7} double mutants. **B)** *BaraA* expression profiles in wild-type, *spz*^{rm7} and *Rel*^{E20} flies upon septic injury with the Gram-negative bacterium *E. coli* and the yeast *C. albicans*. *DptA* and *BomBc3* were used as inducible control genes for the Imd and Toll pathways respectively. Floating asterisks indicate significance relative to *iso-UC* where: * = p < .05 and, *** = p < .001. **C-D)** Use of a *BaraA* reporter (*BaraA-Gal4; UAS-mCD8-GFP* referred to as *BaraA>mGFP*) reveals that *BaraA* is induced upon infection in the fat body of adults **(C)** and in larvae **(D)**. Representative images taken 60h (adults) or 2h (larvae) after handling alone (UC) or infection with *M. luteus* (OD=200). **E-H)** *BaraA>mGFP* is highly expressed in the head and central nervous system **(E)**, behind the eyes and in the ocelli **(F)**, in the wing veins **(G-H** yellow arrows**)**, and beneath the cuticle in the thorax **(H**, orange arrows**)**.

171

Baramicin A encodes a precursor protein cleaved into multiple peptides

Previous studies using bioinformatics and proteomics have suggested that four highly immune-induced peptides (IM10, IM12, IM13, and IM24) are encoded in tandem as a single polypeptide precursor by *IMPPP/BaraA* [8,21]. Some less-abundant sub-peptides (IM5, IM6, and IM8) are also produced by additional cleavage of IM12 and IM13 [21]. Using a newly generated null mutant ("*ΔBaraA,*" described below), we analyzed haemolymph samples of infected wild-type and *ΔBara* flies by MALDI-TOF analysis. We confirmed the loss of the seven immune-induced peaks corresponding to IMs 5, 6, 8, 10, 12, 13, and 24 in *ΔBaraA* flies (**Fig.** 2A). We also noticed that an additional immune-induced peak at ~5975 Da was absent in our *BaraA* mutants. Upon re-visiting the original studies that annotated the *Drosophila* IMs, we realized this peak corresponded to IM22, whose sequence was never determined [8,21] (see supplementary information for details). We subjected immune-induced haemolymph to LC-MS proteomic analysis following trypsin digestion and found that in addition to the known IMs of *BaraA* (IMs 5, 6, 8, 10, 12, 13, and 24), trypsin-digested fragments of the *BaraA* C-terminus peptide were also detectable in the haemolymph (**Fig.** S2). The range of detected fragments did not match the full length of the C-terminus exactly, as the first four residues were absent in our LC-MS data (a truncation not predicted to arise via trypsin cleavage). The *BaraA* C-terminus lacking these four residues has a calculated mass of 5974.5 Da, exactly matching the observed mass of the IM22 peak absent in *BaraA* mutant flies. Furthermore in other *Drosophila* species these four residues of the *BaraA* C-terminus are an RXRR furin cleavage motif (**Fig.** S3A). IM22 cleavage via this motif should produce the same IM22 domain as seen in *D. melanogaster*. Taken together, we conclude that IM22 is the mature form of the BaraA protein C-terminus.

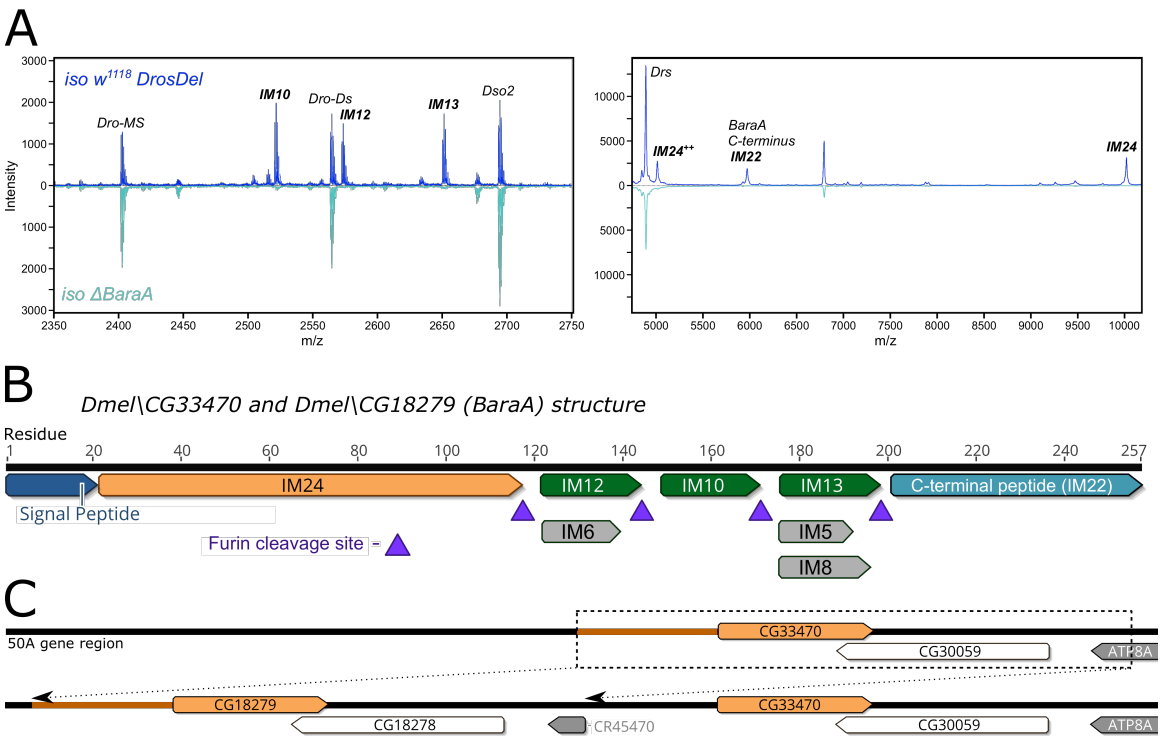

Figure 2: The *Baramicin A* polypeptide genes. A) MALDI-TOF analysis of haemolymph from *iso w*^{1118} wild-type and *iso ΔBaraA* flies 24 hours post-infection (hpi) confirms that *BaraA* mutants fail to produce the IM10-like and IM24 peptides. *iso ΔBaraA* flies also fail to produce an immune-induced peak at ~5794 Da corresponding to IM22 (the C-terminal peptide of BaraA, see supplementary information). **B)** The *BaraA* gene encodes a precursor protein that is cleaved into multiple mature peptides at RXRR furin cleavage sites. The sub-peptides IMs 5, 6, and 8 are additional minor cleavage products of IM12 and IM13. **C)** There is a *BaraA* locus duplication event present in the Dmel_R6 reference genome. This duplication is not fixed in laboratory stocks and wild-type flies (Hanson and Lemaitre; in prep).

Thus, a single gene, *BaraA*, contributes to one third of the originally described IMs. These peptides are encoded as a polypeptide precursor interspersed by furin cleavage sites (e.g. RXRR) (**Fig.** 2B). We note that the IM10, IM12 and IM13 peptides are tandem repeats of related peptides, which we collectively refer to as "IM10-like" peptides (**Fig.** S3B). The IM22 peptide also contains a similar motif as the IM10-like peptides (**Fig.** S3A-B), suggesting a related biological activity. We rename this gene "*Baramicin A*" (symbol: *BaraA*) for the Japanese idiom Bara Bara (バラバラ), meaning "to break apart;" a reference to the fragmenting structure of the *Baramicin* precursor protein and its many peptidic products.

A BaraA duplication is present in several laboratory stocks

Over the course of our investigation, we realized that *IMPPP (CG18279)* was identical to its neighbour gene *CG33470* owing to a duplication event of the *BaraA* locus present in the *D. melanogaster* reference genome. The exact nature of this duplication, and its consequence on the immune response is discussed in a separate article (Hanson and Lemaitre; in prep). In brief, the duplication involves the entire *BaraA* gene including over 1kbp of 100% identical promoter sequence, and also the neighbouring sulfatase gene CG30059 and the 3' terminus of the *ATP8A* gene region (**Fig.** 2C). We distinguish the two daughter genes as *BaraA1 (CG33470)* and *BaraA2 (CG18279).* Available sequence data suggests the *BaraA1* and *BaraA2* transcripts are 100% identical. Interestingly, *BaraA* copy number is variable in common lab strains and wild flies, indicating this duplication event is not fixed in *D. melanogaster* (Hanson and Lemaitre; in prep).

Over-expression of BaraA improves the resistance of immune deficient flies

Imd, Toll deficient flies are extremely susceptible to microbial infection as they fail to induce hundreds of immune genes, including antimicrobial peptides [11]. It has been shown that over-expression of even a single AMP can improve the resistance of *Imd, Toll* deficient flies [22]. As such, immune gene over-expression in *Imd, Toll* immune-compromised flies provides a sensitive assay for testing the ability of a gene to contribute to defence independent of other immune effectors. We applied this strategy to *Baramicin A* by generating flies that constitutively express *BaraA* using the ubiquitous *Actin5C-Gal4* driver in an immune-deficient Rel^{E20}, spz^{rm7} background (**Fig.** 3A). In these experiments, we pooled results from both males and females due to the very low rate of homozygous *Rel, spz* adults, particularly when

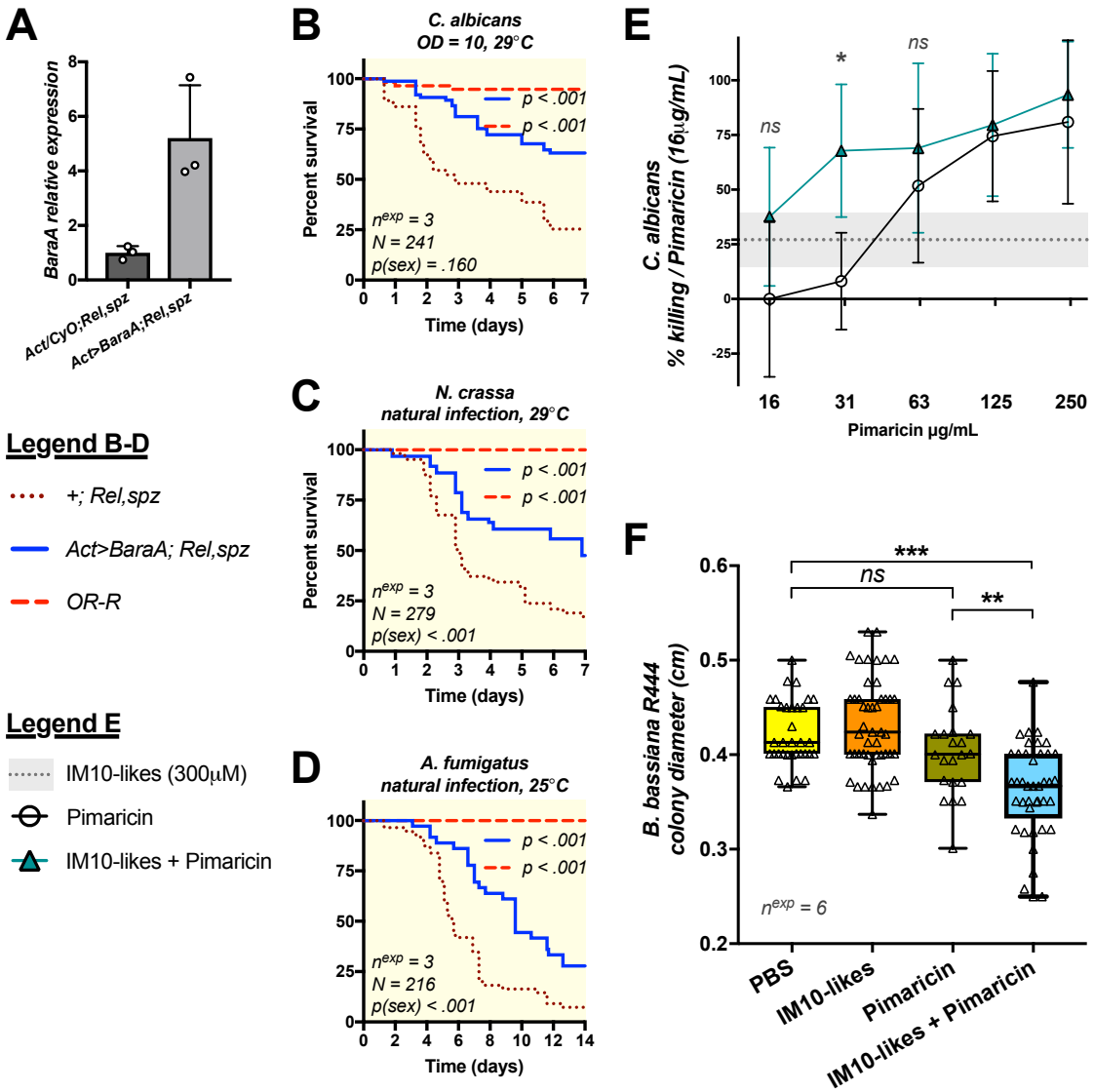

249

Figure 3: Overexpression of *BaraA* partially rescues the susceptibility of *Rel, spz* flies against fungi and BaraA IM10-like peptides inhibit fungal growth in vitro. A) Validation of the *Act>BaraA* construct in unchallenged flies. **B-D)** Overexpression of *BaraA* (*Act>BaraA)* rescues the susceptibility of *Rel, spz* flies upon systemic infection with *C. albicans* **(B)**, or natural infection with either *N. crassa* or *A. fumigatus* **(C-D)**. Survivals represent pooled results from males and females (see **Fig.** S4 for sex-specific survival curves). **E)** A 300µM cocktail of the three IM10-like peptides improves the killing activity of the antifungal Pimaricin against *C. albicans* yeast. Error bars and the shaded area (IM10-likes alone) represent ±1 standard deviation from the mean. Killing activity (%) was compared against no-peptide controls, then normalized to the activity of Pimaricin alone. **F)** The IM10-like peptide cocktail also synergizes with Pimaricin to inhibit mycelial growth of *B. bassiana strain R444*. The diameters of individual colonies of *B. bassiana* were assessed after four days of growth at 29°C after peptide treatment.

250

combined with *Actin-Gal4*. Similar trends were seen in both sexes, and separate male and female survival curves are shown in **Fig.** S4.

Ubiquitous *BaraA* expression marginally improved the survival of *Rel, spz* flies upon bacterial infection with *Pectobacterium carotovora (Ecc15)* and to a lesser extent *M luteus* bacteria, while having no effect on *E. coli* (**Fig. S4A-C**). However, ubiquitous expression of *BaraA* provided a more pronounced protective effect against infection by a variety of fungal pathogens. This was true upon pricking with *C. albicans* (**Fig.** 3B), or upon natural infections using *Aspergillus fumigatus* or *Neurospora crassa* filamentous fungi (**Fig.** 3C-D). This over-expression study reveals that *BaraA* alone can partially rescue the susceptibility of *Imd, Toll* deficient flies to infection, and points to a more prominent role for *BaraA* in antifungal defence.

IM10-like peptides display antifungal activity in vitro

The Baramicin A gene encodes a polypeptide precursor that ultimately produces multiple mature peptides. However the most prominent *BaraA* products are the 23-residue IM10, 12, and 13 peptides (collectively the "IM10-like" peptides); indeed three IM10-like peptides are produced for every one IM24 peptide (**Fig.** 2B), and IM22 also bears an IM10-like motif (**Fig.** S3). This prompted us to explore the in vitro activity of the BaraA IM10-like peptides as potential AMPs.

We synthesized IM10, IM12, and IM13 and performed in vitro antimicrobial assays with these three IM10-like peptides using a 1:1:1 cocktail with a final concentration of 300μM (100 μM each of IM10, IM12, and IM13). Using a protocol adapted from Wiegand et al. [23], we monitored the microbicidal activity of this peptide cocktail either alone, or in combination with membrane-disrupting antibiotics that facilitate peptide entry into the cell. We based this approach on previous studies that showed e.g. that the microbicidal activities of Abaecin-like peptides, which target the bacterial DNA chaperone *DnaK,* increase exponentially in combination with a membrane disrupting agent [24–26]. We did not detect any

killing activity of our IM10-like peptide cocktail alone against *Ecc15, Enterococcus faecalis,* or *C. albicans*. We also found no activity of IM10-like peptides against *Ecc15 or E. faecalis* when co-incubated with a sub-lethal dose of Cecropin or Ampicillin respectively. However, we observed a synergistic interaction between IM10-like peptides and the antifungal Pimaricin against *C. albicans* (**Fig.** 3E). Co-incubation of the IM10-like cocktail with Pimaricin significantly improved the killing activity of Pimaricin at 32μg/mL relative to either treatment alone. While not statistically significant, the combination of IM10-like cocktail and Pimaricin also outperformed either the IM10-like cocktail or Pimaricin alone across the entire range of Pimaricin concentrations tested.

We next co-incubated preparations of *B. bassiana* R444 spores under the same conditions as used previously with *C. albicans*, plated 2μL droplets, and assessed the diameters of colonies derived from individual spores after 4 days of growth at 25°C. We found that neither the IM10-like cocktail nor Pimaricin alone affected colony diameter relative to PBS buffer control alone (Tukey's HSD: p = 0.775 and 0.430 respectively). However in combination, the IM10-like cocktail plus Pimaricin led to significantly reduced colony size compared to either treatment alone (**Fig.** 3F, Tukey's HSD: p = .004). This indicates that incubation with IM10-like peptides and Pimaricin synergistically inhibits *B. bassiana* mycelial growth, revealing an otherwise cryptic antifungal effect of the BaraA IM10-like peptides.

Overall, we found that IM10-like peptides alone do not kill *C. albicans* yeast or impair *B. bassiana* mycelial growth in vitro. However IM10-like peptides seem to synergize with the antifungal Pimaricin to inhibit growth of both of these fungi.

BaraA deficient flies broadly resist as wild type upon bacterial infection

To further characterize *BaraA* function, we generated a null mutation of *BaraA* by replacing the 'entire' *BaraA* locus with a dsRed cassette using CRISPR

mediated homology-directed repair in a w^{1118} genetic background that contains only one *BaraA* gene copy. This mutation ($BaraA^{SW1}$ hereafter "*ΔBaraA"*) was isogenized by seven rounds of backcrossing into the w^{1118} *DrosDel* isogenic genetic background (*iso* w^{1118}) [27] as described in Ferreira et al. [28]. Relevant to this study, both our *iso* w^{1118} and *OR-R* wild type lines contain the duplication and thus have both *BaraA1 and A2* genes, while both copies are absent in *ΔBaraA* flies.

We validated these mutant lines by PCR, qPCR and MALDI-TOF peptidomics (**Fig.** 2A, supplementary data file 1). *BaraA*-deficient flies were viable with no morphological defect. Furthermore, *ΔBaraA* flies have wild-type Toll and Imd signalling responses following infection, indicating that *BaraA* is not required for the activation of these signaling cascades (**Fig.** S5). We next challenged *BaraA* mutant flies using two genetic backgrounds (*w; ΔBaraA* and *iso ΔBaraA*) with a variety of pathogens. We included Imd-deficient Rel^{E20} flies, Toll deficient spz^{rm7} flies and *Bomanin* deficient $Bom^{\Delta 55C}$ flies as positive controls. We observed that *BaraA* null flies have comparable resistance as wild type to infection with the Gram-negative bacteria *Ecc15* or *Providencia burhodogranariea* (**Fig.** S6A-B), or with the Gram-positive bacterium *B. subtilis* (**Fig.** S6C). In contrast, we saw a mild increase in the susceptibility of *w; ΔBaraA* flies to infection by the Gram-positive bacterium *E. faecalis* (HR = +0.73, p = .014), which was consistent in *iso ΔBaraA* flies, although this was not statistically significant (**Fig.** 4A). This mild susceptibility was also observed using flies carrying the *BaraA* mutation over a deficiency (*ΔBaraA/Df(BaraA))*, as well as in flies ubiquitously expressing *BaraA* RNAi (**Fig.** S7); however none of these sets of survival experiments individually reached statistical significance.

BaraA mutant flies are highly susceptible to fungal infection

Entomopathogenic fungi such as *Beauveria bassiana* represent an important class of insect pathogens [6]. They have the ability to directly invade the body cavity

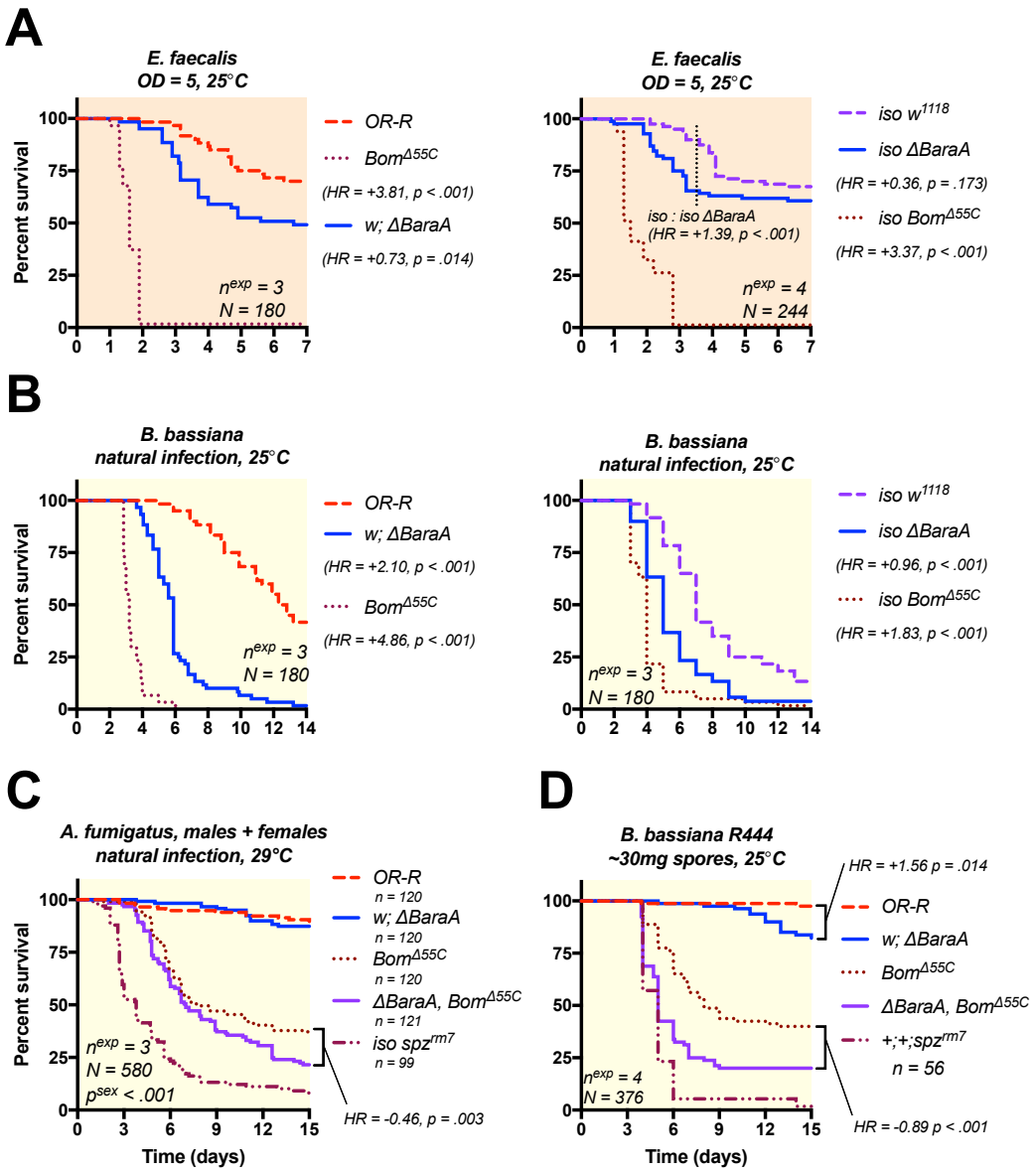

Figure 4: *ΔBaraA* flies are most susceptible to fungal infection. A) *BaraA* mutants with two different genetic backgrounds (here called *w* or *iso*) display a mild susceptibility to systemic infection with *E. faecalis*. This presents as an earlier mortality in the *iso* background (dotted line). However, survival in *iso ΔBaraA* flies was not significantly different from wild type at seven days post-infection (p = .173). **B)** *BaraA* mutants are susceptible to natural infection with the entomopathogenic fungus *B. bassiana*. **C-D)** *ΔBaraA , Bom$^{\Delta 55C}$* double mutant flies were more susceptible to natural infection with *A. fumigatus* **(C)** and *B. bassiana R444* **(D)** than *Bom$^{\Delta 55C}$* single mutant flies (also see **Fig.** S6E-F).

by crossing through the insect cuticle. The Toll pathway is critical to survive fungal pathogens as it is directly responsible for the expression of *Bomanins*, *Daishos*, *Drosomycin* and *Metchnikowin* antifungal effectors [12,14,15,29,30]. The fact that i) *BaraA* is Toll-regulated, ii) BaraA IM10-like peptides have antifungal properties in vitro , and iii) *BaraA* overexpression improves the resistance of *Imd, Toll* deficient flies against fungi all point to a role for *BaraA* against fungal pathogens.

We infected *BaraA* mutants and wild-type flies by rolling flies in sporulating *B. bassiana* petri dishes. Strikingly, both *w; ΔBaraA* and *iso ΔBaraA* flies displayed a pronounced susceptibility to natural infection with *B. bassiana* (HR = +2.10 or +0.96 respectively, $p < .001$ for both) (**Fig.** 4B). An increased susceptibility to fungi was also observed using flies carrying the *BaraA* mutation over a deficiency (**Fig.** S8A) or that ubiquitously express *BaraA* RNAi (**Fig.** S8B). Moreover, constitutive *BaraA* expression (*Act-Gal4>UAS-BaraA)* in an otherwise wild-type background improves survival to *B. bassiana* relative to *Act-Gal4>OR-R* controls (HR = -0.52, $p = .010$) (**Fig.** S8C).

In contrast to the findings with *B. bassiana*, survival analysis revealed only a minor susceptibility of *BaraA* mutants upon infection via injury with *C. albicans* or natural infection with *A. fumigatus* (**Fig.** S6D-F), neither of which reached statistical significance. Collectively, our survival analysis points most strongly to a role for *BaraA* in defence against the entomopathogenic fungus *B. bassiana*.

BaraA contributes to antifungal defence independent of Bomanins

Use of compound mutants carrying multiple mutations in effector genes has shown that some of them additively contribute to host resistance to infection. For instance, *Drosomycin, Metchnikowin* double mutants are more susceptible than single mutants to *C. albicans* [15]. Compound deletions of immune genes can also reveal contributions of immune effectors that are not detectable via single mutant analysis [31,32]. Recent studies have indicated that *Bomanins* play a major role in

383 defence against fungi [12,13], though their mechanism of action is unknown. This
384 prompted us to investigate the interaction of *Bomanins* and *BaraA* in defence against
385 fungi. To do this, we recombined the $Bom^{\Delta 55C}$ mutation (that removes a cluster of 10
386 *Bomanin* genes) with *ΔBaraA.* These *w; ΔBaraA,* $Bom^{\Delta 55C}$ double mutant flies were
387 perfectly viable. While natural infection with *Aspergillus fumigatus* did not induce
388 significant mortality in *BaraA* single mutants, we observed that the combined
389 *ΔBaraA* and $Bom^{\Delta 55C}$ mutations increases fly susceptibility to this pathogen relative
390 to $Bom^{\Delta 55C}$ alone (HR = -0.46, p = .003; **Fig.** 4C).
391
392 We next exposed these *ΔBaraA*, $Bom^{\Delta 55C}$, double mutant flies to 30mg of
393 commercial spores of *B. bassiana R444*, which we found to be a less virulent
394 infection model. This is equivalent to approximately 60 million spores, much of
395 which are removed afterwards upon fly grooming. When using this infection
396 method, we found that *BaraA* mutation markedly increases the susceptibility of *Bom*
397 mutant flies (HR = -0.89, p < .001), approaching spz^{rm7} susceptibility (**Fig.** 4D).
398
399 We conclude that the contribution of *BaraA* to defence does not rely on the
400 presence of *Bomanins*, and vice versa. This finding is consistent with the ability of
401 constitutively expressed *BaraA* to improve survival outcome even in *Imd, Toll*
402 deficient flies. Taken together, these results suggest *BaraA* improves survival
403 against fungi independent of other effectors of the systemic immune response,
404 consistent with a direct effect on invading fungi.
405
406 ***ΔBaraA males display an erect wing phenotype upon infection***
407
408 While performing infections with *A. fumigatus*, we observed a high
409 prevalence of *BaraA* mutant flies with upright wings (**Fig.** 5A-B), a phenotype
410 similar to the effect of disrupting the gene encoding the "*erect wing"* (*ewg*)
411 transcription factor [33]. Curiously, this erect wing phenotype was most specifically
412 observed in males. Upon further observation, erect wing was observed not only
413 upon *A. fumigatus* infection, but also upon infections with all Gram-positive bacteria

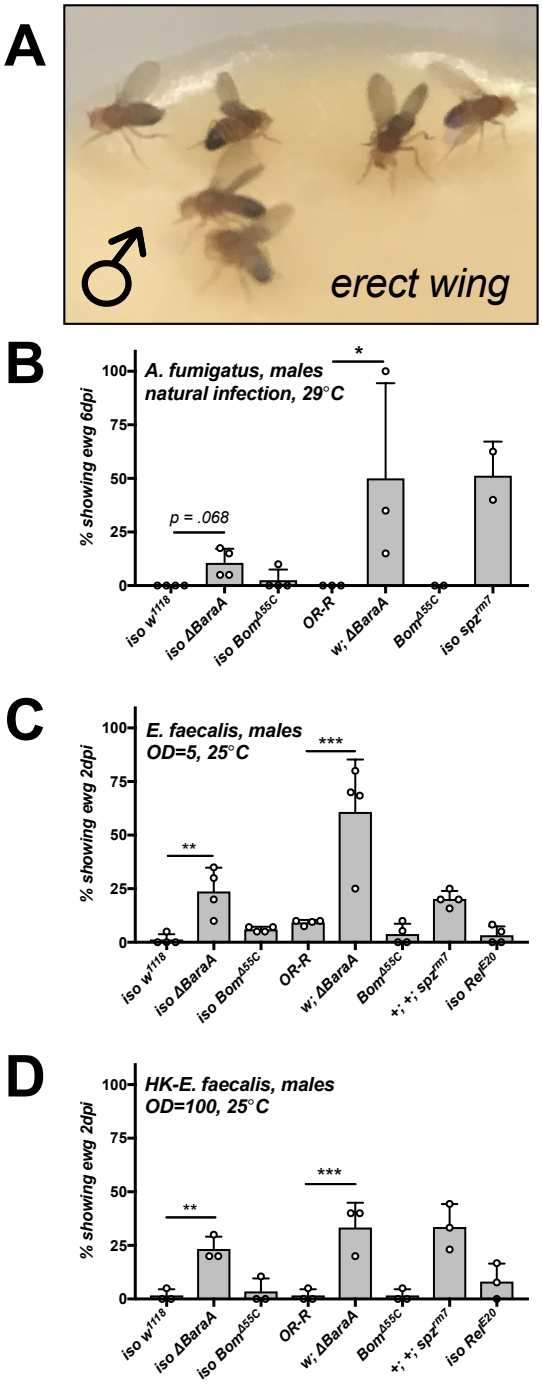

Figure 5: *ΔBaraA* males display an erect wing phenotype upon infection. A) *ΔBaraA* males displaying erect wing six days after *A. fumigatus* natural infection. **B-D)** spz^{rm7} and *ΔBaraA* males, but not $Bom^{\Delta 55C}$ or Rel^{E20} flies display the erect wing phenotype upon natural infection with *A. fumigatus* **(B)**, or septic injury with live **(C)** or heat-killed *E. faecalis* **(D)**. Barplots show the percentage of flies displaying erect wing following treatment, with individual data points reflecting replicate experiments. Additional challenges are shown in Table S1.

and fungi tested (**Table** S1). Increased prevalence of erect wing flies was observed upon infection with both live (**Fig.** 5C) and heat-killed *E. faecalis* (**Fig.** 5D), but less so upon clean injury or via infection with the Gram-negative bacteria *Ecc15*. (**Fig.** S9A-B). Thus, the erect wing phenotype appears to be observed in *BaraA* mutants in response to stimuli known to activate the Toll pathway, but does not require a live infection.

Such a phenotype in infected males has never been reported, but is reminiscent of the wing extension behaviour of flies infected by the brain-controlling "zombie" fungus *Enthomopthera muscae* [34]. Intrigued by this phenotype, we further explored its prevalence in other genetic backgrounds. We next confirmed that this phenotype was also observed in other *BaraA*-deficient backgrounds such as *Df(BaraA)/ΔBara*; however the penetrance was variable from one

439 background to another. Erect wing was also observed in *ΔBaraA*/+ heterozygous
440 flies (*Df(BaraA)/+* or *ΔBaraA*/+), indicating that the lack of one dose of *BaraA* was
441 sufficient to cause the phenotype (**Fig.** S9C and **Table** S1). Moreover, spz^{rm7} flies that
442 lack functional Toll signalling phenocopy *ΔBaraA* flies and display erect wing, but
443 other immune-deficient genotypes such as mutants for the Toll-regulated *Bomanin*
444 effectors ($Bom^{\Delta 55C}$), or Rel^{E20} mutants that lack Imd signalling, do not frequently
445 display erect wing (**Fig.** 5C-D, **Table** S1). Thus the erect wing behaviour is not linked
446 to susceptibility to infection, but rather to loss of *BaraA* upon stimuli triggering the
447 Toll immune pathway. This phenotype suggests an additional effect of *BaraA* on
448 tissues related to the wing muscle or in the nervous system.
449

450 # Discussion (1508 words):

451

452 Seven *Drosophila* AMPs were identified in the 1980's-1990's either by
453 homology with AMPs characterized in other insects or owing to their abundant
454 production and microbicidal activities in vitro [35]. In the 2000s, genome
455 annotations revealed the existence of many additional paralogous genes from the
456 seven well-defined families of AMPs [36,37]. At that time, microarray and MALDI-
457 TOF analyses also revealed the existence of many more small immune-induced
458 peptides, which may function as AMPs [8,21]. Genetic analyses using loss of function
459 mutations have recently shown that some of these peptides do play an important
460 role in host defence, however key points surrounding their direct microbicidal
461 activities remain unclear. In 2015, *Bomanins* were shown to be critical to host
462 defence using genetic approaches, but to date no activity in vitro has been found
463 [12,13]. Two candidate AMPs, Listericin [38] and GNBP-like3 [39], were shown to
464 inhibit microbial growth upon heterologous expression using S2 cell lines or
465 bacteria respectively. Most recently, Daisho peptides were shown to bind to fungal
466 hyphae ex vivo, and are required for resisting fungal infection in vivo [14]. However
467 the mechanism and direct microbicidal activity of these peptides at physiological
468 concentrations was not assessed.

In this study, we provide evidence from four separate experimental approaches that support adding *BaraA* to the list of bona-fide antifungal peptides. First, the *BaraA* gene is strongly induced in the fat body upon infection resulting in abundant peptide production. *BaraA* is also tightly regulated by the Toll pathway, which orchestrates the antifungal response. Second, loss of function study shows that *BaraA* contributes to resistance against various fungi. Our in vivo analyses reveal a potential range of activity for *BaraA* in defence against the yeast *C. albicans*, the mould *A. fumigatus*, and most prominently the entomopathogenic fungus *B. bassiana*; a marginal effect was also seen upon *E. faecalis* bacterial infections. Third, the antifungal activity of *BaraA* is independent of other key effectors. Over-expression of *BaraA* in the absence of other inducible peptides increased resistance of *Imd, Toll* deficient flies to *C. albicans*, *A. fumigatus*, and *N. crassa*. Moreover *BaraA, Bomanin* double mutants suffered greater susceptibility than *Bomanin* mutants alone even against otherwise avirulent fungal pathogens. Lastly, in vitro assays show that a cocktail of the *BaraA* IM10-like peptides possess antifungal activity when co-incubated with the membrane disrupting antifungal Pimaricin.

While it is difficult to estimate the concentration of BaraA peptides in the haemolymph of infected flies, it is expected based on MALDI-TOF peak intensities that the IM10-like peptides should reach concentrations similar to other AMPs (up to 100µM) [10,20]; Our in vitro assays used a peptide cocktail at the upper limit of this range. AMPs are often - but not exclusively – positively charged. This positive charge is thought to recruit these molecules to negatively charged membranes of microbes [10]. However the net charges at pH=7 of the IM10-like peptides are: IM10 +1.1, IM12 +0.1, and IM13 -0.9. Given this range of net charge, IM10-like peptides are not overtly cationic. However some AMPs are antimicrobial without being positively charged, exemplified by human Dermicidin [40] and anionic peptides of Lepidoptera that also synergize with membrane-disrupting agents [41]. However more extensive in vitro experiments with additional fungi should confirm the range

of BaraA peptide activities, and assay the potential activities of IM22 and IM24, which were not included in this study.

Entomopathogenic fungi pose a ubiquitous challenge to insects, and in turn insects use a combination of mechanisms to combat invading fungi. This defence relies largely on humoral factors most notably melanization and the production of host defence peptides. In *Drosophila*, five classes of host defence peptides (plus isoforms) have been shown to contribute to survival against fungi: Drosomycin, Metchnikowin, Bomanins, Daishos, and now the Baramicin A peptides. Additional uncharacterized peptides regulated by the Toll pathway could expand this list further. It interesting to note that *Baramicin* is found conserved throughout the *Drosophila* genus and in closely related outgroup species (Hanson and Lemaitre; in prep) with a species range similar to *Metchnikowin* and *Daisho*. Meanwhile the most well studied antifungal peptide Drosomycin is in fact specific only to *D. melanogaster* and close relatives. While other AMPs such as the antibacterial peptides Attacin, Cecropin, and Defensin, are conserved across Diptera and other insect orders, antifungal peptide genes found in *Drosophila* appear to be younger [14,42]. The presence of these seemingly novel antifungal genes could be one factor that allows *Drosophila* species to exploit such a wide variety of microbe-infested niches compared to more ecologically restricted insect lineages.

Our study also reveals that the *Baramicin A* gene alone produces at least 1/3 of the initially reported IMs. In addition to the IM10-like peptides and IM24 that were previously assigned to *BaraA* [21], we show IM22 is encoded by the C terminus of *BaraA*, and is conserved in other *Drosophila* species. The production of multiple IMs encoded as tandem repeats between furin cleavage sites is built-in to the BaraA protein design akin to a "protein operon." Such tandem repeat organization is rare, but not totally unique among AMPs. This structure was first described in the bumblebee AMP Apidaecin [43], and has since also been found in Drosocin of *Drosophila neotestacea* [44]. In *D. melanogaster*, several AMPs including Attacin C and its pro-peptide MPAC are also furin-processed, and both parts synergize in

killing bacteria [24]. Therefore furin cleavage in Attacin C enables the precise co-expression of distinct peptides with synergistic activity. It is interesting to note that IM10-like peptides did not show antifungal activity in the absence of membrane disruption by Pimaricin. An attractive hypothesis is that longer peptides encoded by BaraA such as IM22 and IM24 could contribute to the antifungal activity of *BaraA* by membrane permeabilization, allowing the internalization of IM10-like peptides. Of note: the IM24 domain is also encoded by two *Baramicin* paralogs named *BaraB* and *BaraC*, which are expressed in the nervous system but do not participate in the inducible immune response (Hanson et al., in prep). This suggests that the IM24 peptidic domain can play a role beyond systemic immunity. The BaraA IM24 peptide is a short Glycine-rich peptide (96 AA) that is positively-charged (charge +2.4 at pH=7). These traits are shared by amphipathic membrane-disrupting AMPs such as Attacins, and also neuropeptides that utilize amphipathic domains to accumulate in neuronal membranes [45]. Thus roles for the Baramicin IM24 domain in both immunity and neurology are not mutually exclusive.

An unexpected observation of our study is the display of an erect wing phenotype by *BaraA* deficient males upon infection. Our study suggests that this is not a consequence of the genetic background, but rather relies on the activation of the Toll pathway in the absence of *BaraA*. The *erect wing* gene, whose inactivation causes a similar phenotype, is a transcription factor that regulates synaptic growth in developing neuromuscular junctions [33]. This raises the intriguing hypothesis that immune processes downstream of the Toll ligand Spaetzle-somehow affect wing neuromuscular junctions, and that *BaraA* modulates this activity. Another puzzling observation is the sexual dimorphism exhibited for this response. It should be noted that male courtship and aggression displays involve similar wing extension behaviours. Koganezawa et al. [46] showed that males deficient for *Gustatory receptor 32a (Gr32a)* failed to unilaterally extend wings during courtship display. *Gr32a*-expressing cells extend into the subesophageal ganglion where they contact mAL, a male-specific set of interneurons involved in unilateral wing display [46]. As erect wing is male-specific, we speculate this *BaraA*-mediated effect might rely on

interactions with such male-specific neurons. *BaraA* is highly produced in the fat body upon infection but also expressed in the nervous system. Further studies should decipher whether the preventative effect of *BaraA* on the erect wing phenotype is cell autonomous or linked to BaraA peptides secreted into the haemolymph. Erect wing is also induced by heat-killed bacteria, and is not observed in *Bomanin* or *Relish* mutants, indicating that the erect wing phenotype is not a generic consequence of susceptibility to infection. Recent studies have highlighted how NF-κB signalling in the brain is activated by bacterial peptidoglycan [47], and that immune effectors expressed either by fat body surrounding the brain or from within brain tissue itself affect memory formation [39]. Moreover, an AMP of nematodes regulates aging-dependent neurodegeneration through binding to its G-protein coupled receptor, and this pathway is sufficient to trigger neurodegeneration following infection [48]. Thus immune-inducible AMPs can have striking interactions with neurological processes. Future studies characterizing the role of *BaraA* in the erect wing phenotype should provide insight on interactions between systemic immunity and host physiology.

Here we describe a complex immune effector gene that produces multiple peptide products. *BaraA* encodes many of the most abundant immune effectors induced downstream of the Toll signalling pathway, and indeed *BaraA* promotes survival upon fungal infection. How each peptide contributes to the immune response and/or erect wing behaviour will be informative in understanding the range of effects immune effectors can have on host physiology. This work and others also clarifies how the cocktail of immune effectors produced upon infection acts specifically during innate host defence reactions.

Materials and methods:

Fly genetics and sequence comparisons

Sequence files were collected from FlyBase [49] and recently-generated sequence data [44,50] and comparisons were made using Geneious R10. Putative NF-κB binding sites were annotated using the Relish motif "GGRDNNHHBS" described in Copley et al. [18] and a manually curated amalgam motif of "GGGHHNNDVH" derived from common Dif binding sites described previously [17,19]. Gene expression analyses were performed using primers described in **Supplementary data file 1**, and further microarray validation for *BaraA* expression comes from De Gregorio et al. [11].

The *UAS-BaraA* and *BaraA-Gal4* constructs were generated using the TOPO pENTR entry vector and cloned into the pTW or pBPGUw Gateway™ vector systems respectively. The *BaraA-Gal4* promoter contains 1675bp upstream of *BaraA1* (but also *BaraA2,* sequence in supplementary information). The *BaraA-Gal4* construct was inserted into the VK33 attP docking site (BDSC line #24871). The $BaraA^{SW1}$ (*ΔBaraA)* mutant was generated using CRISPR with two gRNAs and an HDR vector by cloning 5' and 3' region-homologous arms into the pHD-dsRed vector, and consequently *ΔBaraA* flies express dsRed in their eyes, ocelli, and abdomen. *ΔBaraA* was generated in the Bloomington stock BL51323 as this background contains only one copy of the *BaraA* locus. The induction of the immune response in these flies was validated by qPCR and MALDI-TOF proteomics, wherein we discovered an aberrant *Dso2* locus in the BL51323 background. We thus backcrossed the *ΔBaraA* mutation once with a standard w^{1118} background and screened for wild-type *Dso2* before use in any survival experiments. Additionally, *ΔBaraA* was isogenized into the *DrosDel* w^{1118} isogenic background for seven generations before use in isogenic fly experiments as described in Ferreira et al. [28].

A full description of fly stocks used for crosses and in experiments is provided in **Supplementary data file 1**.

Microbe culturing conditions

Bacteria and *C. albicans* yeast were grown to mid-log phase shaking at 200rpm in their respective growth media (LB, BHI, or YPG) and temperature conditions, and then pelleted by centrifugation to concentrate microbes. Resulting cultures were diluted to the desired optical density at 600nm (OD) for survival experiments as indicated. The following microbes were grown at 37°C: *Escherichia coli strain 1106* (LB), *Enterococcus faecalis* (BHI), and *Candida albicans* (YPG). The following microbes were grown at 29°C: *Erwinia carotovora carotovora (Ecc15)* (LB) and *Micrococcus luteus* (LB). For filamentous fungi and molds, *Aspergillus fumigatus* was grown at 37°C, and *Neurospora crassa* and *Beauveria bassiana* were grown at room temperature on Malt Agar in the dark until sporulation. *Beauveria bassiana strain R444* commercial spores were produced by Andermatt Biocontrol, product BB-PROTEC.

Survival experiments

Survival experiments were performed as previously described [15], with 20 flies per vial with 2-3 replicate experiments. 3-5 day old males were used in experiments unless otherwise specified. For fungi natural infections, flies were flipped at the end of the first day to remove excess fungal spores from the vials. Otherwise, flies were flipped thrice weekly. Statistical analyses were performed using a Cox proportional hazards (CoxPH) model in R 3.6.3. We report the hazard ratio (HR) alongside p-values as a proxy for effect size in survival experiments. Throughout our analyses, we required $p < .05$ as evidence to report an effect as significant, but note interactions with $|HR| > 0.5$ as potentially important provided α approached .05, and tamp down importance of interactions that were significant, but have relatively minor effect size ($|HR| < 0.5$).

Erect wing scoring

651 The erect wing phenotype was scored as the number of flies with splayed
652 wings throughout a distinct majority of the period of observation (30s); if unclear,
653 the vial was monitored an additional 30s. Here we define splayed wings as wings
654 not at rest over the back, but did not require wings to be fully upright; on occasion
655 wings were held splayed outward at ~45° relative to the dorsal view, and often
656 slightly elevated relative to the resting state akin to male aggressive displays.
657 Sometimes only one wing was extended, which occurred in both thoracic pricking
658 and fungi natural infections; these flies were counted as having erect wing. In
659 natural infections, the typical course of erect wing display developed in two fashions
660 at early time points, either: i) flies beginning with wings slightly splayed but not
661 fully upright, or ii) flies constantly flitting their wings outward and returning them
662 to rest briefly, only to flit them outward again for extended periods of time. Shortly
663 after infection, some flies were also observed wandering around with wings beating
664 at a furious pace, which was not counted as erect wing. However at later time points
665 erect wing flies settled more permanently on upright splayed wings. Erect wing
666 measurements were taken daily following infection, and erect wing flies over total
667 flies was converted to a percent. Data points in **Fig.** 5B-D represent % with erect
668 wing in individual replicate experiments with ~20 flies per vial. Flies stuck in the
669 vial, or where the wings had become sticky or mangled were not included in totals.
670 **Table** S1 reports mean percentages across replicate experiments for all pathogens
671 and genotypes where erect wing was monitored. Days post-infection reported in
672 **Table** S1 were selected as the final day prior to major incidents of mortality. For *E.*
673 *faecalis* live infections, $Bom^{\Delta 55C}$ and spz^{rm7} erect wing was taken at 1dpi due to major
674 mortality events by 2dpi specifically in these lines.
675
676 Erect wing measurements were performed in parallel with survival
677 experiments, which often introduced injury to the thorax below the wing possibly
678 damaging flight muscle. It is unlikely that muscle damage explains differences in
679 erect wing display. First: we noticed erect wing initially during natural infections
680 with *A. fumigatus*, and observed erect wing upon *B. bassiana R444* and *Metarhizium*

rileyi PHP1705 natural infections (**Table** S1; *M. rileyi* = NOMU-PROTEC, Andermatt Biocontrol). Second: only 1 of 75 total *iso* w^{1118} males displayed erect wing across 4 systemic infection experiments with *E. faecalis*. For comparison: 19 of 80 total *iso ΔBaraA* and 48 of 80 *w; ΔBaraA* flies displayed erect wing (**Table** S1). Future studies might be better served using an abdominal infection mode, which can have different infection dynamics [51]. However we find erect wing display to be robust upon either septic injury or natural infection modes.

IM10-like peptide in vitro activity

The 23-residue Baramicin peptides were synthesized by GenicBio to a purity of >95%, verified by HPLC. An N-terminal pyroglutamate modification was included based on previous peptidomic descriptions of Baramicins IM10, IM12, and IM13 [52], which we also detected in our LC-MS data (**Fig.** S2). Peptides were dissolved in DMSO and diluted to a working stock of 1200μM in 0.6% DMSO; the final concentration for incubations was 300μM in 0.15% DMSO. For microbe-killing assays, microbes were allowed to grow to log-growth phase, at which point they were diluted to ~50cells/μL. Two μL of culture (~100 cells), and 1μL water or antibiotic was mixed with 1μL of a 1:1:1 cocktail of IM10, IM12, and IM13 peptides to a final concentration of 300μM total peptides; 1μL of water + DMSO (final concentration = 0.15% DMSO) was used as a negative control. Four μL microbe-peptide solutions were incubated for 24h at 4°C. Microbe-peptide cultures were then diluted to a final volume of 100μL and the entire solution was plated on LB agar or BiGGY agar plates. Colonies were counted manually. For combinatorial assays with bacteria, *C. albicans* yeast, and *B. bassiana R444* spores, peptide cocktails were combined with membrane disrupting antimicrobials effective against relevant pathogens beginning at: 10 μM Cecropin A (Sigma), 500μg/mL ampicillin, or 250μg/mL Pimaricin (commercially available as "Fungin," InVivogen), serially diluted through to 0.1 μM, 0.5μg/mL, and 4μg/mL respectively.

Beauveria bassiana R444 spores were prepared by dissolving ~30mg of spores in 10mL PBS, and then 4µL microbe-peptide solutions were prepared as described for *C. albicans* followed by incubation for 24h at 4°C; this spore density was optimal in our hands to produce distinct individual colonies. Then, 4µL PBS was added to each solution and 2µL droplets were plated on malt agar at 25°C. Colony diameters were measured 4 days after plating by manually analyzing images. Experimental replicates were included as co-variates in One-way ANOVA analysis. The initial dataset approached violating Shapiro-Wilk assumptions of normality ($p = 0.061$) implemented in R 3.6.3. We subsequently removed four colonies from the analysis, as these outliers were over two standard deviations lower than their respective mean (removed colonies: PBS 0.15cm, PBS 0.25cm, IM10-like+Pimaricin 0.21cm, and a second IM10-like+Pimaricin colony of 0.21cm); the resulting Shapiro-Wilk p-value = 0.294, and both QQ and residual plots suggested a normal distribution. Final killing activities and colony diameters were compared by One-way ANOVA with Holm-Sidak multiple test correction (*C. albicans*) and Tukey's honest significant difference multiple test correction (*B. bassiana R444*).

Gene expression analyses

RNA was extracted using TRIzol according to manufacturer's protocol. cDNA was reverse transcribed using Takara Reverse Transcriptase. qPCR was performed using PowerUP mastermix from Applied Biosystems at 60°C using primers listed in **Supplementary data file 1**. Gene expression was quantified using the PFAFFL method [53] with *Rp49* as the reference gene. Statistical analysis was performed by One-way ANOVA with Holm-Sidak's multiple test correction or student's t-test. Error bars represent one standard deviation from the mean.

Proteomic analyses

740 Raw haemolymph samples were collected from immune-challenged flies for
741 MALDI-TOF proteomic analysis as described in [14,15]. MALDI-TOF proteomic
742 signals were confirmed independently at facilities in both San Diego, USA and
743 Lausanne, CH. In brief, haemolymph was collected by capillary and transferred to
744 0.1% TFA before addition to acetonitrile universal matrix. Representative spectra
745 are shown. Peaks were identified via corresponding m/z values from previous
746 studies [8,21]. Spectra were visualized using mMass, and figures were additionally
747 prepared using Inkscape v0.92.
748
749 **Author contributions:**
750
751 MAH planned experiments, performed bioinformatic analyses, infection
752 experiments, and in vitro assays. BL supervised the project and MAH and BL wrote
753 the manuscript. LC planned and generated the *BaraA* deletion and performed key
754 descriptive experiments and observations. AM assisted with infection and in vitro
755 assays. II, and SAW generated and supplied critical reagents and provided
756 constructive commentary.
757
758 **Acknowledgements:**
759
760 This research was supported by Sinergia grant CRSII5_186397 and Novartis
761 Foundation 532114 awarded to Bruno Lemaitre, and by National Institute of Health
762 (NIH) grant R01 GM050545 to Steven Wasserman. We thank Jean-Philippe Boquete
763 for assistance with the generation of Gal4 and UAS constructs. We would also like to
764 acknowledge the technical expertise provided by the proteomics and mass
765 spectrometry facilities in both UCSD and EPFL, and specifically Adrien Schmid. The
766 name "*Baramicin*" was partly inspired by Eichero Oda's character "Buggy," a Bara-
767 Bara superhuman. Finally, we further thank Huang et al. (*in preparation*) for their
768 cooperation in publishing initial descriptions of the *BaraA* gene, and for stimulating
769 discussion.
770

References:

1. Lemaitre B, Hoffmann J. The Host Defense of Drosophila Melanogaster. Annual Review of Immunology. 2007;25: 697–743. doi:10.1146/annurev.immunol.25.022106.141615

2. Kurz CL, Ewbank JJ. Caenorhabditis elegans: An emerging genetic model for the study of innate immunity. Nature Reviews Genetics. 2003;4: 380–390. doi:10.1038/nrg1067

3. Kaufmann SHE. Immunology's foundation: the 100-year anniversary of the Nobel Prize to Paul Ehrlich and Elie Metchnikoff. Nat Immunol. 2008;9: 705–712. doi:10.1038/ni0708-705

4. Steiner H, Hultmark D, Engström \AA, Bennich H, Boman HG. Sequence and specificity of two antibacterial proteins involved in insect immunity. Nature. 1981;292: 246–248. doi:10.1038/292246a0

5. Lemaitre B, Nicolas E, Michaut L, Reichhart JM, Hoffmann JA. The dorsoventral regulatory gene cassette spatzle/Toll/Cactus controls the potent antifungal response in Drosophila adults. Cell. 1996;86: 973–983. doi:10.1016/S0092-8674(00)80172-5

6. Lemaitre B, Reichhart JM, Hoffmann JA. Drosophila host defense: differential induction of antimicrobial peptide genes after infection by various classes of microorganisms. Proceedings of the National Academy of Sciences of the United States of America. 1997;94: 14614–9. doi:10.1073/pnas.94.26.14614

7. Lemaitre B, Kromer-Metzger E, Michaut L, Nicolas E, Meister M, Georgel P, et al. A recessive mutation, immune deficiency (imd), defines two distinct control pathways in the Drosophila host defense. Proc Natl Acad Sci U S A. 1995;92: 9465–9469. doi:10.1073/pnas.92.21.9465

8. Uttenweiler-Joseph S, Moniatte M, Lagueux M, Van Dorsselaer a, Hoffmann J a, Bulet P. Differential display of peptides induced during the immune response of Drosophila: a matrix-assisted laser desorption ionization time-of-flight mass spectrometry study. Proceedings of the National Academy of Sciences of the United States of America. 1998;95: 11342–11347. doi:10.1073/pnas.95.19.11342

9. Lazzaro BP, Zasloff M, Rolff J. Antimicrobial peptides: Application informed by evolution. Science. 2020;368. doi:10.1126/science.aau5480

10. Hanson MA, Lemaitre B. New insights on Drosophila antimicrobial peptide function in host defense and beyond. Curr Opin Immunol. 2020;62: 22–30. doi:10.1016/j.coi.2019.11.008

11. De Gregorio E, Spellman PT, Tzou P, Rubin GM, Lemaitre B. The Toll and Imd pathways are the major regulators of the immune response in Drosophila. EMBO Journal. 2002;21: 2568–2579. doi:10.1093/emboj/21.11.2568

12. Clemmons AW, Lindsay SA, Wasserman SA. An Effector Peptide Family Required for Drosophila Toll-Mediated Immunity. PLoS Pathogens. 2015;11. doi:10.1371/journal.ppat.1004876

13. Lindsay SA, Lin SJH, Wasserman SA. Short-Form Bomanins Mediate Humoral Immunity in Drosophila. 2018. doi:10.1159/000489831

14. Cohen LB, Lindsay SA, Xu Y, Lin SJH, Wasserman SA. The Daisho Peptides Mediate Drosophila Defense Against a Subset of Filamentous Fungi. Front Immunol. 2020;11: 9. doi:10.3389/fimmu.2020.00009

15. Hanson MA, Dostálová A, Ceroni C, Poidevin M, Kondo S, Lemaitre B. Synergy and remarkable specificity of antimicrobial peptides in vivo using a systematic knockout approach. eLife. 2019;8. doi:10.7554/elife.44341

16. Unckless RL, Howick VM, Lazzaro BP. Convergent Balancing Selection on an Antimicrobial Peptide in Drosophila. Current Biology. 2016;26: 257–262. doi:10.1016/j.cub.2015.11.063

17. Busse MS, Arnold CP, Towb P, Katrivesis J, Wasserman SA. A κB sequence code for pathway-specific innate immune responses. EMBO Journal. 2007;26: 3826–3835. doi:10.1038/sj.emboj.7601798

18. Copley RR, Totrov M, Linnell J, Field S, Ragoussis J, Udalova IA. Functional conservation of Rel binding sites in drosophilid genomes. Genome Research. 2007;17: 1327–1335. doi:10.1101/gr.6490707

19. Tanji T, Yun E-Y, Ip YT. Heterodimers of NF-κB transcription factors DIF and Relish regulate antimicrobial peptide genes in Drosophila. Proceedings of the National Academy of Sciences. 2010;107: 14715–14720. doi:10.1073/pnas.1009473107

20. Ferrandon D, Jung AC, Criqui MC, Lemaitre B, Uttenweiler-Joseph S, Michaut L, et al. A drosomycin-GFP reporter transgene reveals a local immune response in Drosophila that is not dependent on the Toll pathway. EMBO Journal. 1998;17: 1217–1227. doi:10.1093/emboj/17.5.1217

21. Levy F, Rabel D, Charlet M, Bulet P, Hoffmann JA, Ehret-Sabatier L. Peptidomic and proteomic analyses of the systemic immune response of Drosophila. Biochimie. 2004;86: 607–616. doi:10.1016/j.biochi.2004.07.007

22. Tzou P, Reichhart J-M, Lemaitre B. Constitutive expression of a single antimicrobial peptide can restore wild-type resistance to infection in immunodeficient Drosophila mutants. Proceedings of the National Academy of Sciences of the United States of America. 2002;99: 2152–2157. doi:10.1073/pnas.042411999

23. Wiegand I, Hilpert K, Hancock REW. Agar and broth dilution methods to determine the minimal inhibitory concentration (MIC) of antimicrobial substances. Nature Protocols. 2008. doi:10.1038/nprot.2007.521

24. Rabel D, Charlet M, Ehret-Sabatier L, Cavicchioli L, Cudic M, Otvos L, et al. Primary Structure and in Vitro Antibacterial Properties of the Drosophila melanogaster Attacin C Pro-domain. Journal of Biological Chemistry. 2004;279: 14853–14859. doi:10.1074/jbc.M313608200

25. Rahnamaeian M, Cytry ska M, Zdybicka-Barabas A, Dobslaff K, Wiesner J, Twyman RM, et al. Insect antimicrobial peptides show potentiating functional interactions against Gram-negative bacteria. Proceedings of the Royal Society B: Biological Sciences. 2015;282: 20150293–20150293. doi:10.1098/rspb.2015.0293

26. Kragol G, Lovas S, Varadi G, Condie BA, Hoffmann R, Otvos L. The antibacterial peptide pyrrhocoricin inhibits the ATPase actions of DnaK and prevents chaperone-assisted protein folding. Biochemistry. 2001;40: 3016–3026. doi:10.1021/bi002656a

27. Ryder E, Blows F, Ashburner M, Bautista-Llacer R, Coulson D, Drummond J, et al. The DrosDel collection: A set of P-element insertions for generating custom chromosomal aberrations in Drosophila melanogaster. Genetics. 2004;167: 797–813. doi:10.1534/genetics.104.026658

28. Ferreira ÁG, Naylor H, Esteves SS, Pais IS, Martins NE, Teixeira L. The Toll-dorsal pathway is required for resistance to viral oral infection in Drosophila. PLoS Pathog. 2014;10: e1004507. doi:10.1371/journal.ppat.1004507

29. Levashina EA, Ohresser S, Bulet P, Reichhart J -M, Hetru C, Hoffmann JA. Metchnikowin, a Novel Immune-Inducible Proline-Rich Peptide from Drosophila with Antibacterial and Antifungal Properties. European Journal of Biochemistry. 1995;233: 694–700. doi:10.1111/j.1432-1033.1995.694_2.x

30. Fehlbaum P, Bulet P, Michaut L, Lagueux M, Broekaert WF, Hetru C, et al. Insect immunity: Septic injury of drosophila induces the synthesis of a potent

antifungal peptide with sequence homology to plant antifungal peptides. Journal of Biological Chemistry. 1994;269: 33159–33163.

31. Dudzic JP, Hanson MA, Iatsenko I, Kondo S, Lemaitre B. More Than Black or White: Melanization and Toll Share Regulatory Serine Proteases in Drosophila. Cell Reports. 2019;27: 1050–1061.e3. doi:10.1016/j.celrep.2019.03.101

32. Binggeli O, Neyen C, Poidevin M, Lemaitre B. Prophenoloxidase Activation Is Required for Survival to Microbial Infections in Drosophila. PLoS Pathogens. 2014;10. doi:10.1371/journal.ppat.1004067

33. DeSimone SM, White K. The Drosophila erect wing gene, which is important for both neuronal and muscle development, encodes a protein which is similar to the sea urchin P3A2 DNA binding protein. Mol Cell Biol. 1993;13: 3641–3649. doi:10.1128/MCB.13.6.3641

34. Elya C, Lok TC, Spencer QE, McCausland H, Martinez CC, Eisen M. Robust manipulation of the behavior of Drosophila melanogaster by a fungal pathogen in the laboratory. eLife. 2018;7: e34414. doi:10.7554/eLife.34414

35. Imler J-L, Bulet P. Antimicrobial peptides in Drosophila: structures, activities and gene regulation. Chemical immunology and allergy. 2005;86: 1–21. doi:10.1159/000086648

36. Hedengren M, Borge K, Hultmark D. Expression and evolution of the Drosophila attacin/diptericin gene family. Biochemical and biophysical research communications. 2000;279: 574–81. doi:10.1006/bbrc.2000.3988

37. Khush RS, Lemaitre B. Genes that fight infection: what the Drosophila genome says about animal immunity. Trends Genet. 2000;16: 442–449. doi:10.1016/s0168-9525(00)02095-3

38. Goto A, Yano T, Terashima J, Iwashita S, Oshima Y, Kurata S. Cooperative regulation of the induction of the novel antibacterial Listericin by peptidoglycan recognition protein LE and the JAK-STAT pathway. J Biol Chem. 2010;285: 15731–15738. doi:10.1074/jbc.M109.082115

39. Barajas-azpeleta R, Wu J, Gill J, Welte R. Antimicrobial peptides modulate long-term memory. PLoS Genetics. 2018; 1–26. doi:10.1371/journal.pgen.1007440

40. Steffen H, Rieg S, Wiedemann I, Kalbacher H, Deeg M, Sahl H-G, et al. Naturally processed dermicidin-derived peptides do not permeabilize bacterial membranes and kill microorganisms irrespective of their charge. Antimicrob Agents Chemother. 2006;50: 2608–2620. doi:10.1128/AAC.00181-06

41. Zdybicka-Barabas A, Mak P, Klys A, Skrzypiec K, Mendyk E, Fiołka MJ, et al. Synergistic action of Galleria mellonella anionic peptide 2 and lysozyme against

913 Gram-negative bacteria. Biochim Biophys Acta. 2012;1818: 2623–2635.
914 doi:10.1016/j.bbamem.2012.06.008

915 42. Hanson MA, Lemaitre B, Unckless RL. Dynamic Evolution of Antimicrobial
916 Peptides Underscores Trade-Offs Between Immunity and Ecological Fitness.
917 Frontiers in Immunology. 2019;10: 2620. doi:doi: 10.3389/fimmu.2019.02620

918 43. Casteels-Josson K, Capaci T, Casteels P, Tempst P. Apidaecin multipeptide
919 precursor structure: a putative mechanism for amplification of the insect
920 antibacterial response. The EMBO journal. 1993;12: 1569–78.
921 doi:10.1002/j.1460-2075.1993.tb05801.x

922 44. Hanson MA, Hamilton PT, Perlman SJ. Immune genes and divergent
923 antimicrobial peptides in flies of the subgenus Drosophila. BMC evolutionary
924 biology. 2016;16: 228. doi:10.1186/s12862-016-0805-y

925 45. Brogden KA, Guthmiller JM, Salzet M, Zasloff M. The nervous system and innate
926 immunity: The neuropeptide connection. Nature Immunology. 2005. pp. 558–
927 564. doi:10.1038/ni1209

928 46. Koganezawa M, Haba D, Matsuo T, Yamamoto D. The Shaping of Male Courtship
929 Posture by Lateralized Gustatory Inputs to Male-Specific Interneurons. Current
930 Biology. 2010;20: 1–8. doi:10.1016/j.cub.2009.11.038

931 47. Kurz CL, Charroux B, Chaduli D, Viallat-Lieutaud A, Royet J. Peptidoglycan
932 sensing by octopaminergic neurons modulates Drosophila oviposition. Elife.
933 2017;6. doi:10.7554/eLife.21937

934 48. Lezi E, Zhou T, Koh S, Chuang M, Sharma R, Pujol N, et al. An Antimicrobial
935 Peptide and Its Neuronal Receptor Regulate Dendrite Degeneration in Aging
936 and Infection. Neuron. 2018;97: 125-138.e5. doi:10.1016/j.neuron.2017.12.001

937 49. Gramates LS, Marygold SJ, Dos Santos G, Urbano JM, Antonazzo G, Matthews BB,
938 et al. FlyBase at 25: Looking to the future. Nucleic Acids Research. 2017;45:
939 D663–D671. doi:10.1093/nar/gkw1016

940 50. Hill T, Koseva BS, Unckless RL. The genome of Drosophila innubila reveals
941 lineage-specific patterns of selection in immune genes. Molecular Biology and
942 Evolution. 2019. doi:10.1093/molbev/msz059

943 51. Chambers MC, Jacobson E, Khalil S, Lazzaro BP. Thorax injury lowers resistance
944 to infection in Drosophila melanogaster. Infect Immun. 2014;82: 4380–4389.
945 doi:10.1128/IAI.02415-14

946 52. Verleyen P, Baggerman G, D'Hertog W, Vierstraete E, Husson SJ, Schoofs L.
947 Identification of new immune induced molecules in the haemolymph of

Drosophila melanogaster by 2D-nanoLC MS/MS. Journal of Insect Physiology. 2006;52: 379–388. doi:10.1016/j.jinsphys.2005.12.007

53. Pfaffl MW. A new mathematical model for relative quantification in real-time RT-PCR. Nucleic Acids Res. 2001;29: e45. doi:10.1093/nar/29.9.e45

54. Tyler-Cross R, Schirch V. Effects of amino acid sequence, buffers, and ionic strength on the rate and mechanism of deamidation of asparagine residues in small peptides. J Biol Chem. 1991;266: 22549–22556.

Supplemental figure captions:

Figure S1: A-F) AMP and *BaraA* expression dynamics upon injury with a mixture of *E. coli* and *M. luteus* (A,D,E,F) and natural infection with *B. bassiana* (B,C), from De Gregorio et al. (2002). **A)** *BaraA* immediate expression dynamics are more similar to *Drs* (Toll and some Imd) than *BomBc3* (Toll-specific). **B)** Natural infection by *B. bassiana* results in sustained *BaraA* expression for days. **C)** Fungus-induced *BaraA* expression is abolished in spz^{rm7} mutants. **D-E)** *BaraA* is induced by bacteria in Rel^{E20} mutants **(D)**, but far less in spz^{rm7} mutants **(E)**. **F)** *BaraA* induction is completely abolished in *Rel, spz* double mutants. **G)** 400bp of upstream sequence from *BaraA* annotated with putative *Rel* or *Dif/dl* binding sites (included in supplemental data file 1). **H)** Expression of *BaraA in wild-type* and spz^{rm7} *flies* following injury with the Gram-positive bacteria *M. luteus* . **I)** The *BaraA>mGFP* reporter line shows more robust induction of GFP 60hpi by pricking with *M. luteus* than *E. coli*. **J)** Expression of *BaraA>mGFP* in the spermatheca of females (yellow arrow). Representative images shown.

Figure S2: LCMS coverage of trypsin-digested and detected BaraA peptides aligned to the protein coding sequence. Peptide fragments cover the whole precursor protein barring furin site-associated motifs. Additionally, two peptide fragments are absent: i) the first 4 residues of the C-terminus ("GIND," not predicted *a priori*), and ii) the C-terminus peptide's "RPDGR" motif, which is predicted as a degradation product of Trypsin cleavage and whose size is beyond the minimum range of detection. Without the GIND motif, the mass of the contiguous C-terminus is 5974.5 Da, matching the mass observed by MALDI-TOF for IM22 (**Fig.** 2A). The N-terminal Q residues of IM10, IM12, IM13, and IM24 are pyroglutamate-modified, as described previously [2]. The asparagine residues of IM10-like peptides are sometimes deamidated, likely as a consequence of our 0.1% TFA sample collection method as "NG" motifs are deamidated in acidic conditions [54].

Figure S3: A) Aligned IM22 peptides of *Drosophila Baramicin A-like* genes, with the IM10-like 'VWKRPDGRTV' motif noted. The GIND residues at the N-terminus are cleaved off in *Dmel\BaraA*, and this site is similarly cleaved at RXRR furin cleavage site in subgenus Drosophila flies. **B)** Alignment of the three IM10-like peptides of *D. melanogaster BaraA* with the "VXRPXRTV" motif noted.

Figure S4: *Over-expression of BaraA partially* rescues *Rel, spz* double mutant susceptibility to infection in both males and females. A) Overexpressing *BaraA* modestly improves survival of *Rel, spz* flies upon injury with *Ecc15*, though initial mortality closely resembles that of *Rel, spz* controls, and the differences observed in males were not significant (p = .106). **B)** Overexpressing *BaraA* did not improve the survival of *Rel, spz* flies upon *E. coli* infection. **C)** Overexpressing *BaraA* only marginally improves survival of *Rel, spz* females, but not males, upon *M. luteus* infections. Infections using a higher dose tended to kill 100% of *Rel, spz* flies regardless of sex or expression of *BaraA*, suggesting that if *BaraA* overexpression

does affect susceptibility to *M. luteus*, this effect is possible within only a narrow window of *M. luteus* concentration. **D-F)** Overexpressing *BaraA* improves survival of *Rel, spz* male and female flies upon injury with *C. albicans* **(D)** or natural infection with *A. fumigatus* **(E)** and *N. crassa* **(F).** P-values are shown for each biological sex in an independent CoxPH model not including the other sex relative to *Rel, spz* as a reference.

Figure S5: RT-qPCR shows that the expression of *BomBc3* **(A)** *Drs* **(B)** and *DptA* **(C)** in wild-type 18hpi in *iso ΔBaraA* flies.

Figure S6: Additional survivals using *ΔBaraA* flies in two distinct genetic backgrounds upon infection by a diversity of microbes. A) No significant susceptibility of *ΔBaraA* flies to *Ecc15* infection. **B)** *iso ΔBaraA* but not *w; ΔBaraA* flies are susceptible to *P. burhodogranariea*, **C)** *w; ΔBaraA but not iso ΔBaraA* flies exhibit a minor susceptibility to *B. subtilis* (HR > 0.5, p = .099). **D)** Both *w; ΔBaraA* and *iso ΔBaraA* exhibit a minor increased susceptibility to *C. albicans*, though the ultimate survival rate was not significantly different from their respective wild-types. Dotted line indicates CoxPH statistical signature when censored at 2dpi. **E-F)** *w; ΔBaraA* males are slightly susceptible to *A. fumigatus* natural infection (HR > 0.5, p = .078), but not females, nor isogenic flies. Additional infections using *ΔBaraA, Bom$^{\Delta 55C}$* double mutant flies reveal that *BaraA* mutation increases the susceptibility of *Bom$^{\Delta 55C}$* flies in both males and females (cumulative curves shown in **Fig.** 4C). Blue backgrounds = Gram-negative bacteria, orange backgrounds = Gram-positive bacteria, yellow backgrounds = fungi.

Figure S7: Additional survival analyses reveal only a minor contribution of *BaraA* to defence against infection by *E. faecalis*. A) Crossing with a genomic deficiency (*Df(BaraA)*) leads to increased susceptibility in both the *w* background and isogenic DrosDel background, with *Df(BaraA)/ΔBaraA* flies suffering the greatest mortality in either crossing scheme. Both deficiency crosses yielded an earlier susceptibility in *BaraA*-deficient flies (shown with dotted black lines), however neither experiment ultimately reached statistical significance. **B)** *BaraA* RNAi flies (*Act>BaraA-IR*) suffered greater mortality than *Act>OR-R* or *OR-R/BaraA-IR* controls, but this was not statistically significant at α = .05.

Figure S8: Additional survival analyses reveal a consistent contribution of *BaraA* to defence against natural infection with *B. bassiana*. A) Crossing with a genomic deficiency (*Df(BaraA)*) leads to increased susceptibility of *Df(BaraA)/ΔBaraA* flies for both the *w* background and isogenic DrosDel background relative to wild-type controls (p < .05). **B)** *Act>BaraA-IR* flies were more susceptible than *OR>BaraA-IR* (p = .004), although not significantly different from our *Act>OR-R* control (p = .266). **C)** Overexpressing *BaraA* (*Act>UAS-BaraA*) improved survival against *B. bassiana* relative to *Act>OR-R* controls (HR = -0.52, p = 0.010).

Figure S9: Frequency of erect wing display following additional challenges. A-B) Erect wing frequencies 2dpi after clean injury **(A)**, or *Ecc15* septic injury **(B)**. The erect wing frequencies of flies pricked by HK-*E. faecalis* (**Fig.** 6D) are overlaid in the background to facilitate direct comparison with the frequency observed upon Toll pathway activation. **C)** The frequency of erect wing display is increased following *E. faecalis* septic injury in *ΔBaraA/+* or *Df(BaraA)/+* flies. Data points are pooled from *w; ΔBaraA* and *iso ΔBaraA* crosses after *E. faecalis* infections shown in **Fig.** S7A and data in **Table** S1.

Table S1: Erect wing frequencies from various infection experiments. Following initial erect wing observations upon *A. fumigatus* natural infection, we scored erect wing frequency in all subsequent survival experiments. Data represent the mean % of males displaying erect wing ± one standard deviation. n exp = number of replicate experiments performed, and dpi ewg taken = days post-infection where erect wing data were recorded. We additionally performed natural infections with *Metarhizium rileyi* that generally did not cause significant mortality in flies, but nevertheless induced erect wing specifically in *ΔBaraA* males and spz^{rm7} controls. Bacterial infections were performed by septic injury, while fungal challenges were natural infections performed by rolling flies in spores.

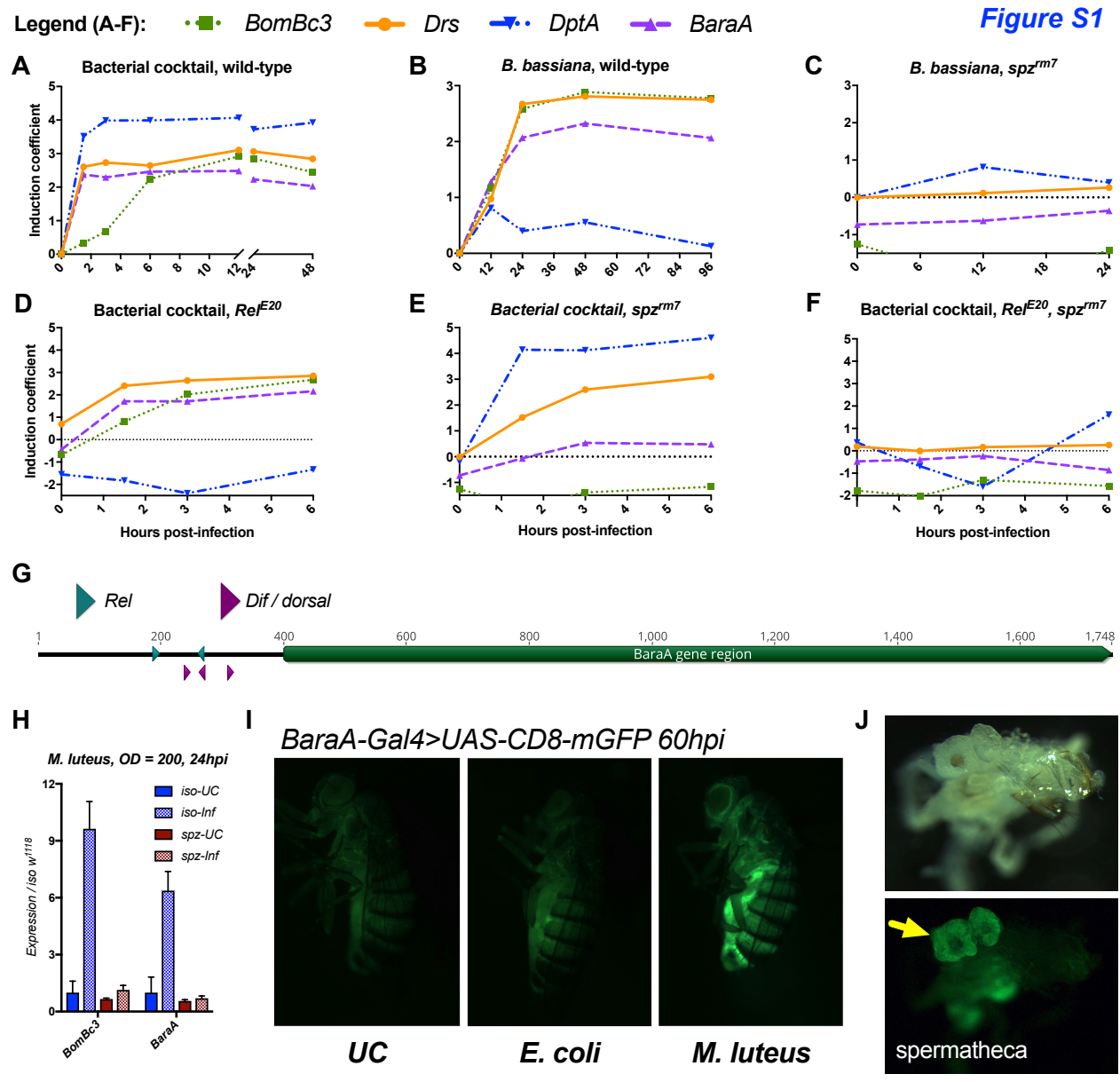
Legend (A-F): BomBc3 Drs DptA BaraA
Figure S1
A
Bacterial cocktail, wild-type
Induction coefficient
B
B. bassiana, wild-type
C
B. bassiana, spzrm7
D
Bacterial cocktail, RelE20
Induction coefficient
Hours post-infection
E
Bacterial cocktail, spzrm7
Hours post-infection
F
Bacterial cocktail, RelE20, spzrm7
Hours post-infection
G
Rel
Dif / dorsal
1
200
400
600
800
1,000
1,200
1,400
1,600
1,748
BaraA gene region
H
M. luteus, OD = 200, 24hpi
iso-UC
iso-Inf
spz-UC
spz-Inf
Expression / iso w1118
BomBc3
BaraA
I
BaraA-Gal4>UAS-CD8-mGFP 60hpi
UC
E. coli
M. luteus
J
spermatheca

Figure S2

A *Figure S3*

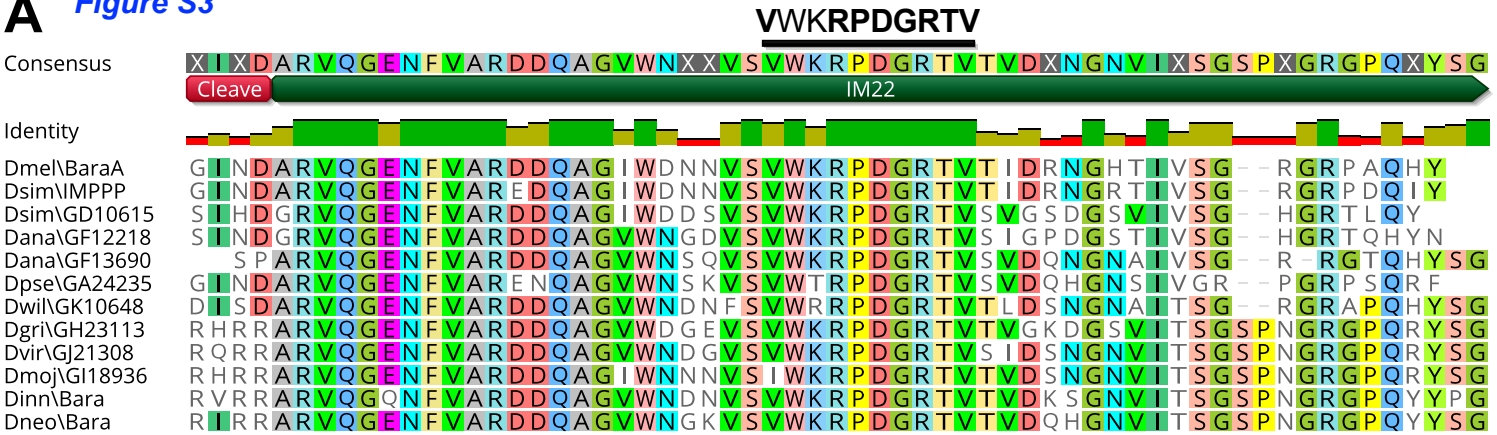
VWKRPDGRTV
Consensus
Cleave
IM22
Identity
Dmel\BaraA
Dsim\IMPPP
Dsim\GD10615
Dana\GF12218
Dana\GF13690
Dpse\GA24235
Dwil\GK10648
Dgri\GH23113
Dvir\GJ21308
Dmoj\GI18936
Dinn\Bara
Dneo\Bara

B


VXRPXRTV
Consensus
Identity
IM12
IM13
IM10

Legend A-F: +; Rel, spz — Act>BaraA; Rel, spz — OR-R

Figure S4

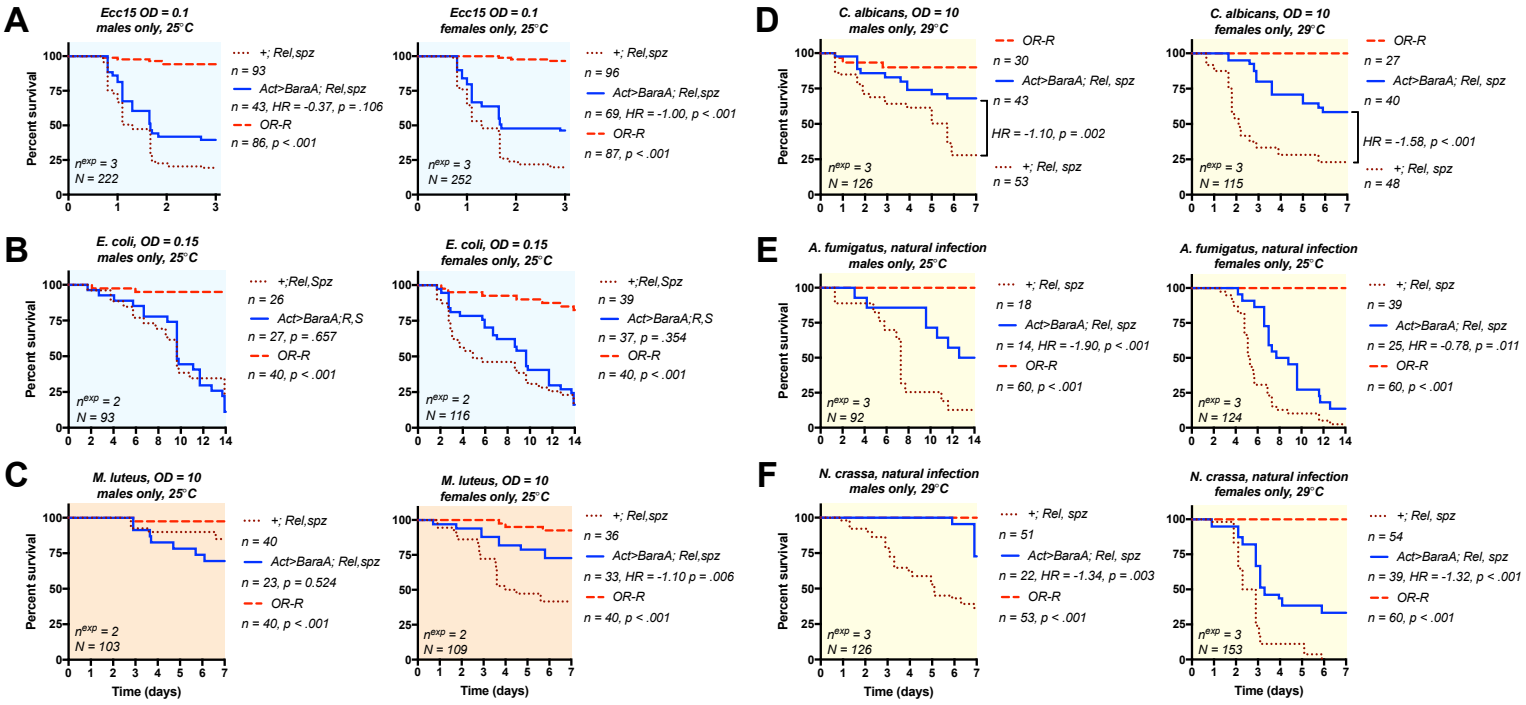

Figure S5

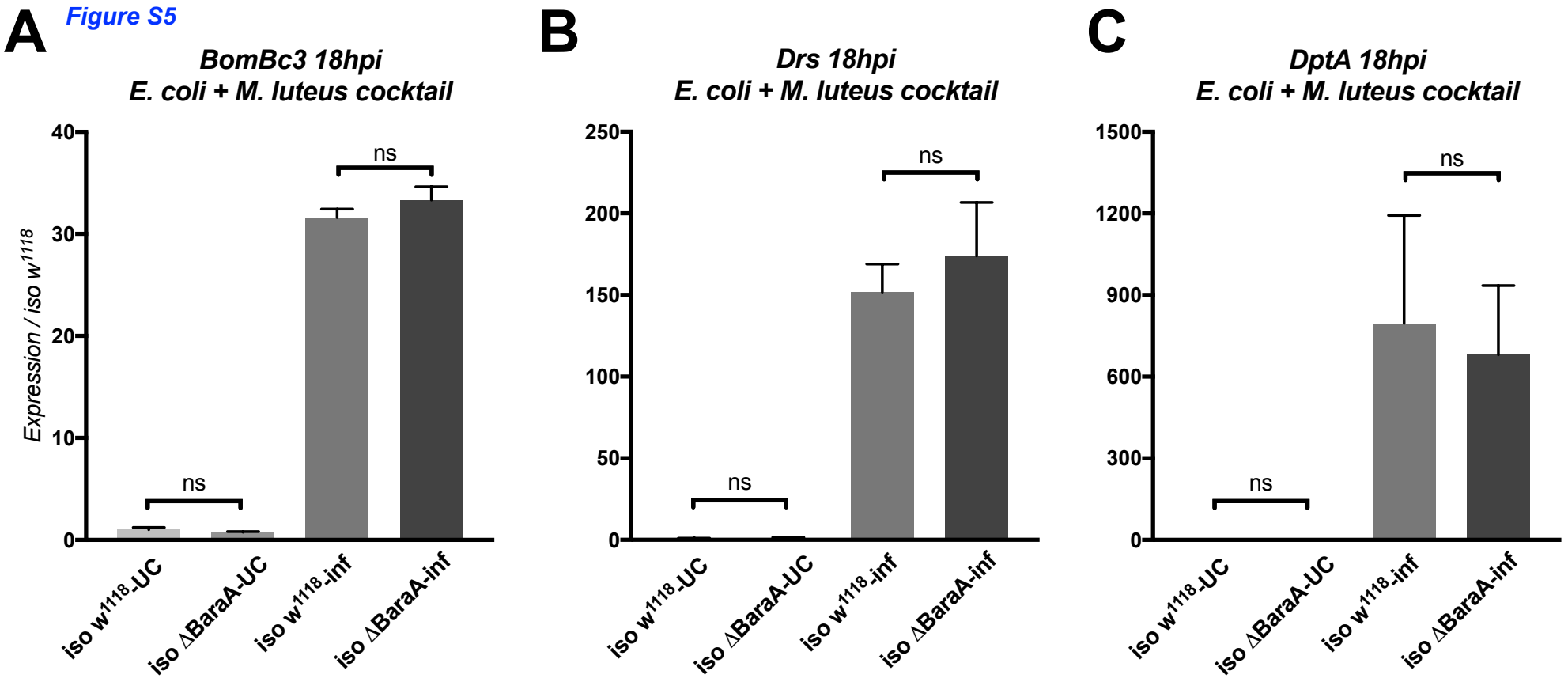
A
BomBc3 18hpi
E. coli + M. luteus cocktail
Expression / iso w1118
40
30
20
10
0
ns
ns
iso w1118-UC
iso ΔBaraA-UC
iso w1118-inf
iso ΔBaraA-inf
B
Drs 18hpi
E. coli + M. luteus cocktail
250
200
150
100
50
0
ns
ns
iso w1118-UC
iso ΔBaraA-UC
iso w1118-inf
iso ΔBaraA-inf
C
DptA 18hpi
E. coli + M. luteus cocktail
1500
1200
900
600
300
0
ns
ns
iso w1118-UC
iso ΔBaraA-UC
iso w1118-inf
iso ΔBaraA-inf

Figure S6

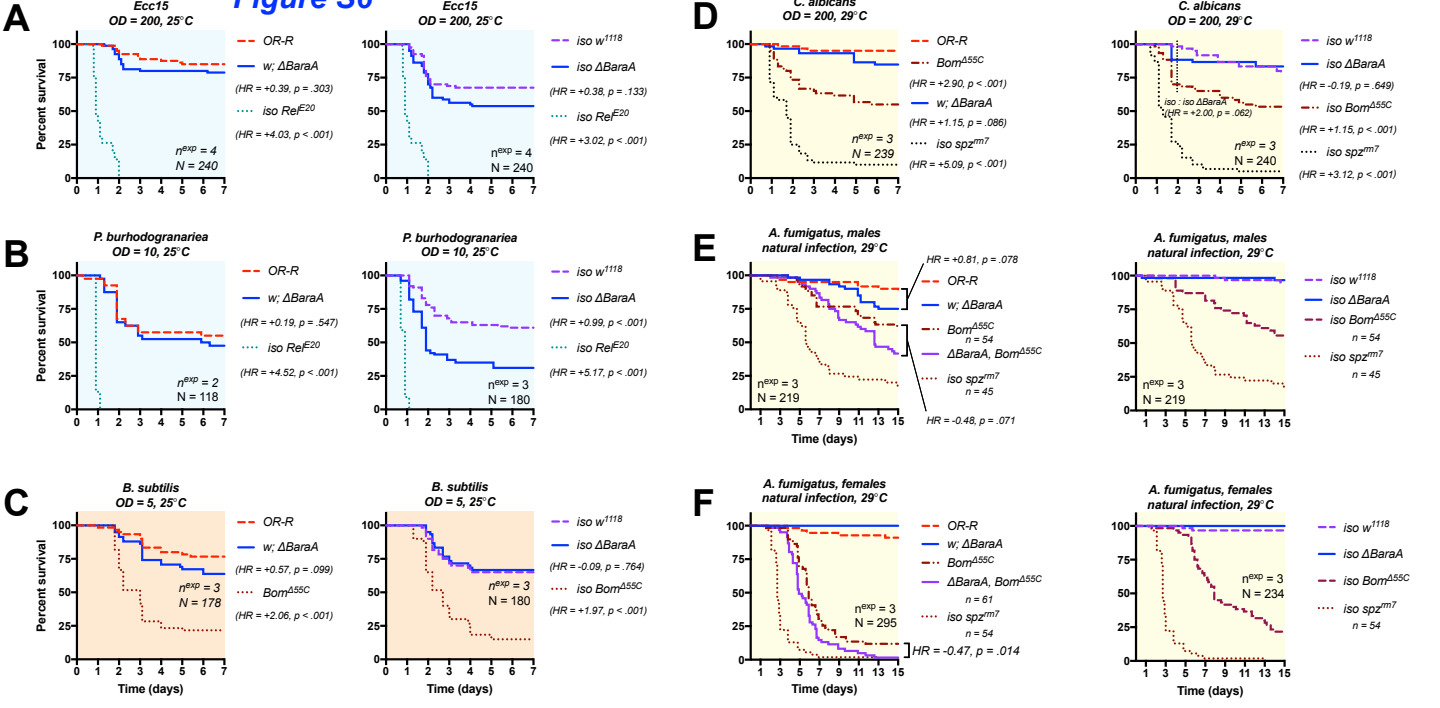
A
Ecc15
OD = 200, 25°C
Percent survival
OR-R
w; ΔBaraA
(HR = +0.39, p = .303)
iso Rel^E20
(HR = +4.03, p < .001)
n^exp = 4
N = 240
Ecc15
OD = 200, 25°C
iso w^1118
iso ΔBaraA
(HR = +0.38, p = .133)
iso Rel^E20
(HR = +3.02, p < .001)
n^exp = 4
N = 240
B
P. burhodogranariea
OD = 10, 25°C
OR-R
w; ΔBaraA
(HR = +0.19, p = .547)
iso Rel^E20
(HR = +4.52, p < .001)
n^exp = 2
N = 118
P. burhodogranariea
OD = 10, 25°C
iso w^1118
iso ΔBaraA
(HR = +0.99, p < .001)
iso Rel^E20
(HR = +5.17, p < .001)
n^exp = 3
N = 180
C
B. subtilis
OD = 5, 25°C
OR-R
w; ΔBaraA
(HR = +0.57, p = .099)
Bom^Δ55C
(HR = +2.06, p < .001)
n^exp = 3
N = 178
Time (days)
B. subtilis
OD = 5, 25°C
iso w^1118
iso ΔBaraA
(HR = -0.09, p = .764)
iso Bom^Δ55C
(HR = +1.97, p < .001)
n^exp = 3
N = 180
Time (days)
D
C. albicans
OD = 200, 29°C
OR-R
Bom^Δ55C
(HR = +2.90, p < .001)
w; ΔBaraA
(HR = +1.15, p = .086)
iso spz^rm7
(HR = +5.09, p < .001)
n^exp = 3
N = 239
C. albicans
OD = 200, 29°C
iso w^1118
iso ΔBaraA
(HR = -0.19, p = .649)
iso Bom^Δ55C
(HR = +1.15, p < .001)
iso spz^rm7
(HR = +3.12, p < .001)
iso : iso ΔBaraA
(HR = +2.00, p = .062)
n^exp = 3
N = 240
E
A. fumigatus, males
natural infection, 29°C
HR = +0.81, p = .078
OR-R
w; ΔBaraA
Bom^Δ55C
n = 54
ΔBaraA, Bom^Δ55C
iso spz^rm7
n = 45
HR = -0.48, p = .071
n^exp = 3
N = 219
Time (days)
A. fumigatus, males
natural infection, 29°C
iso w^1118
iso ΔBaraA
iso Bom^Δ55C
n = 54
iso spz^rm7
n = 45
n^exp = 3
N = 219
F
A. fumigatus, females
natural infection, 29°C
OR-R
w; ΔBaraA
Bom^Δ55C
ΔBaraA, Bom^Δ55C
n = 61
iso spz^rm7
n = 54
HR = -0.47, p = .014
n^exp = 3
N = 295
Time (days)
A. fumigatus, females
natural infection, 29°C
iso w^1118
iso ΔBaraA
iso Bom^Δ55C
iso spz^rm7
n = 54
n^exp = 3
N = 234
Time (days)

Figure S7

A

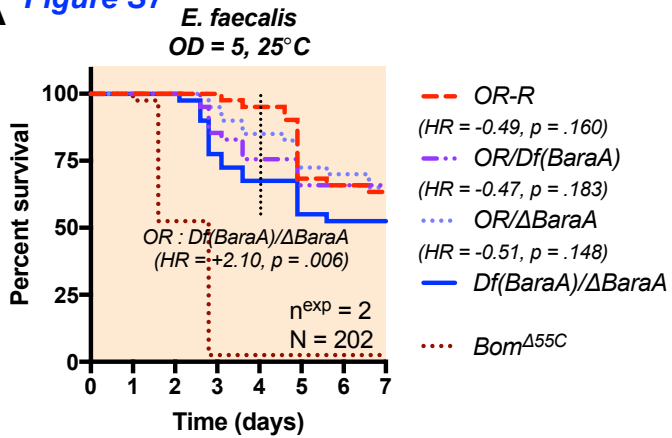
E. faecalis
OD = 5, 25°C
Percent survival
Time (days)
OR : Df(BaraA)/ΔBaraA
(HR = +2.10, p = .006)
n^exp = 2
N = 202
OR-R
(HR = -0.49, p = .160)
OR/Df(BaraA)
(HR = -0.47, p = .183)
OR/ΔBaraA
(HR = -0.51, p = .148)
Df(BaraA)/ΔBaraA
Bom^Δ55C

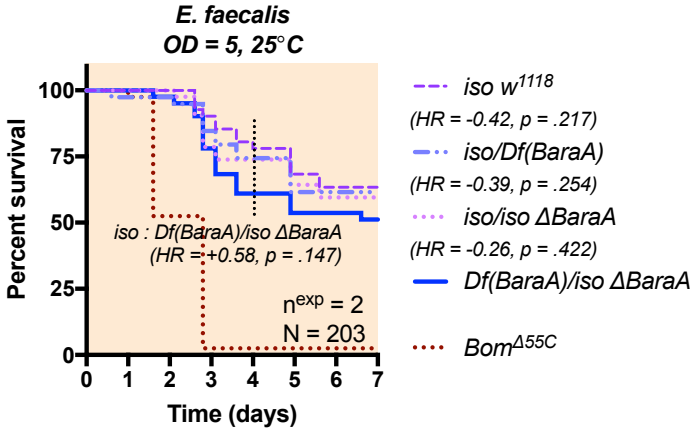
E. faecalis
OD = 5, 25°C
Percent survival
Time (days)
iso : Df(BaraA)/iso ΔBaraA
(HR = +0.58, p = .147)
n^exp = 2
N = 203
iso w^1118
(HR = -0.42, p = .217)
iso/Df(BaraA)
(HR = -0.39, p = .254)
iso/iso ΔBaraA
(HR = -0.26, p = .422)
Df(BaraA)/iso ΔBaraA
Bom^Δ55C

B

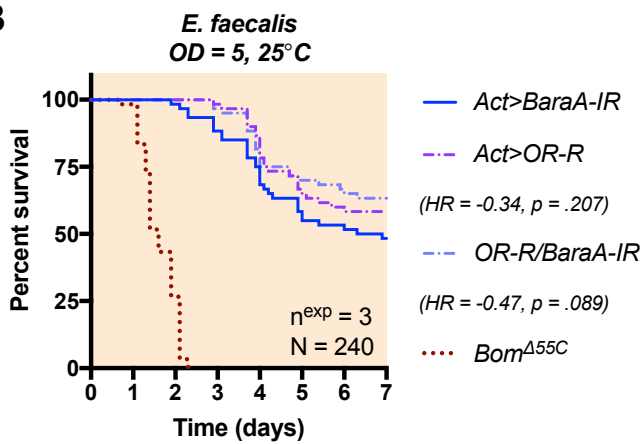
E. faecalis
OD = 5, 25°C
Percent survival
Time (days)
n^exp = 3
N = 240
Act>BaraA-IR
Act>OR-R
(HR = -0.34, p = .207)
OR-R/BaraA-IR
(HR = -0.47, p = .089)
Bom^Δ55C

Figure S8

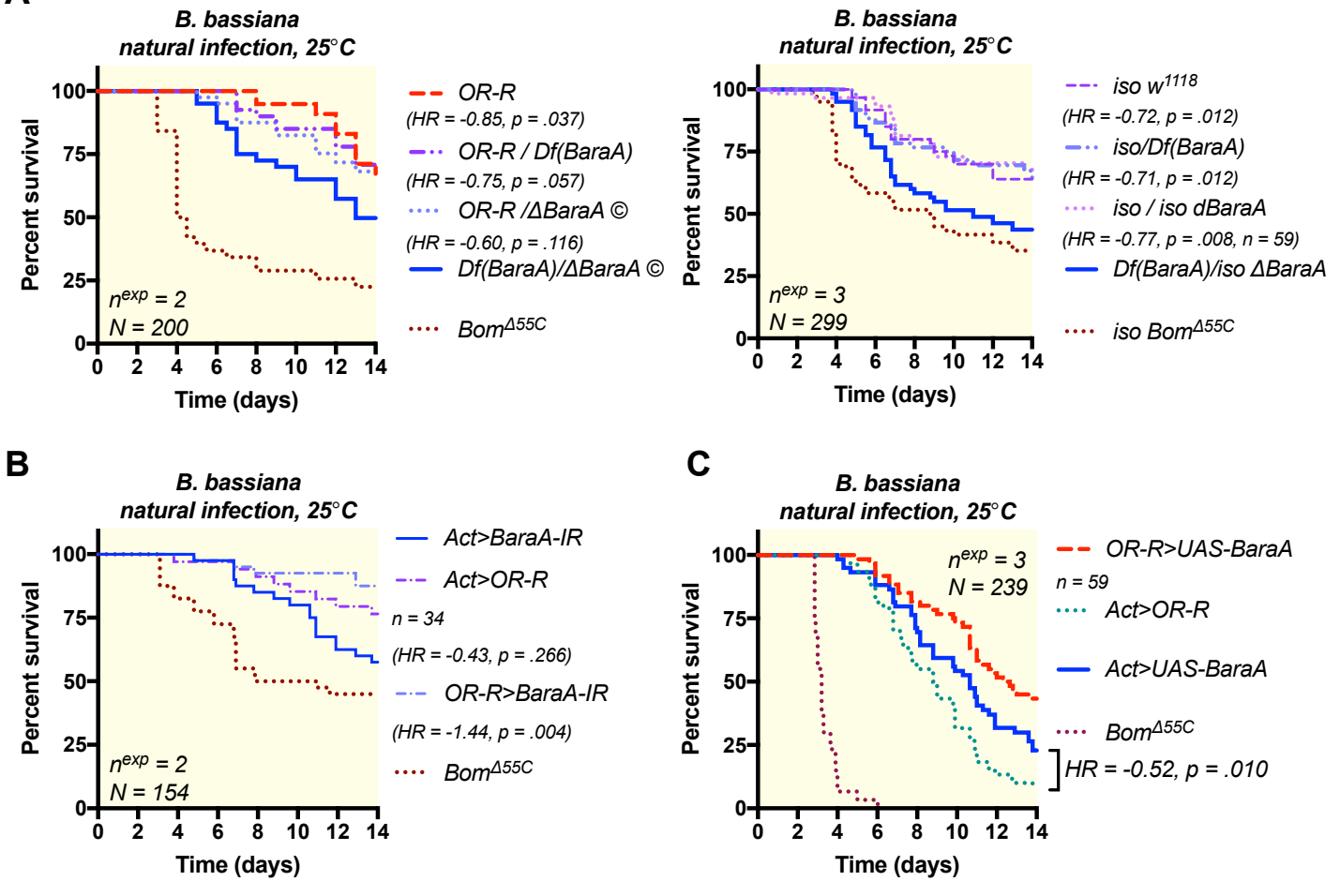
A
B. bassiana
natural infection, 25°C
Percent survival
Time (days)
n^exp = 2
N = 200
OR-R
(HR = -0.85, p = .037)
OR-R / Df(BaraA)
(HR = -0.75, p = .057)
OR-R /ΔBaraA ©
(HR = -0.60, p = .116)
Df(BaraA)/ΔBaraA ©
Bom^Δ55C
B. bassiana
natural infection, 25°C
Percent survival
Time (days)
n^exp = 3
N = 299
iso w^1118
(HR = -0.72, p = .012)
iso/Df(BaraA)
(HR = -0.71, p = .012)
iso / iso dBaraA
(HR = -0.77, p = .008, n = 59)
Df(BaraA)/iso ΔBaraA
iso Bom^Δ55C
B
B. bassiana
natural infection, 25°C
Percent survival
Time (days)
n^exp = 2
N = 154
Act>BaraA-IR
Act>OR-R
n = 34
(HR = -0.43, p = .266)
OR-R>BaraA-IR
(HR = -1.44, p = .004)
Bom^Δ55C
C
B. bassiana
natural infection, 25°C
Percent survival
Time (days)
n^exp = 3
N = 239
OR-R>UAS-BaraA
n = 59
Act>OR-R
Act>UAS-BaraA
Bom^Δ55C
HR = -0.52, p = .010

Figure S9

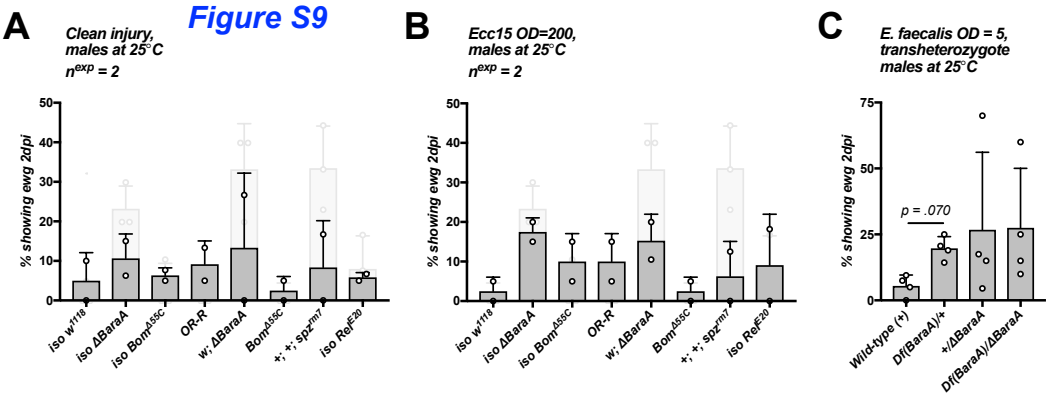
A
Clean injury, males at 25°C
n^exp = 2
% showing ewg 2dpi
50
40
30
20
10
0
iso w^1118
iso ΔBaraA
iso Bom^Δ55C
OR-R
w; ΔBaraA
Bom^Δ55C
+; +; spz^rm7
iso Rel^E20
B
Ecc15 OD=200, males at 25°C
n^exp = 2
% showing ewg 2dpi
50
40
30
20
10
0
iso w^1118
iso ΔBaraA
iso Bom^Δ55C
OR-R
w; ΔBaraA
Bom^Δ55C
+; +; spz^rm7
iso Rel^E20
C
E. faecalis OD = 5, transheterozygote males at 25°C
% showing ewg 2dpi
75
50
25
0
p = .070
Wild-type (+)
Df(BaraA)/+
+/ΔBaraA
Df(BaraA)/ΔBaraA

Table S1

Treatment			***Percent (%) males showing ewg***									
Pathogen	**n exp**	**dpi ewg taken**	***iso DrosDel***	***iso ΔBaraA***	***iso Bom$^{\Delta 55C}$***	***iso spz^{rm7}***	***OR-R***	***w; ΔBaraA***	***Bom$^{\Delta 55C}$***	***+; +; spz^{rm7}***	***iso Rel^{E20}***	***Bom$^{\Delta 55C}$, ΔBaraA***
Clean Injury	2	2	5.0 ± 7.1	10.6 ± 6.2	6.3 ± 1.9		9.2 ± 5.9	13.3 ± 18.9	2.6 ± 3.7	8.3 ± 11.2	5.8 ± 1.2	
HK-E. faecalis (OD100)	3	2	1.7 ± 2.9	23.3 ± 5.8	3.5 ± 6.1		1.7 ± 2.9	33.3 ± 11.6	1.7 ± 2.9	33.6 ± 10.1	8.1 ± 8.3	
E. faecalis (OD5)	4	2	1.3 ± 2.5	23.8 ± 11.1	6.1 ± 1.2		10.5 ± 3.2	60.9 ± 24.4	3.8 ± 4.8	20.2 ± 3.8	3.4 ± 4.1	
B. subtilis	1	2	0.0	30.0	5.0		25.0	40.0	5.0			
A. fumigatus	4 or indicated	6	0.0 ± 0.0	10.6 ± 6.6	2.5 ± 5.0	51.3 ± 15.9 (n=2)	0.0 ± 0.0 (n=3)	50 ± 44.5 (n=3)	0.0 ± 0.0 (n=2)			5.0 ± 7.1 (n=2)
B. bassiana (sporulating plate)	3	3	10.0 ± 0.0	31.5 ± 24.5	11.5 ± 16.0							
B. bassiana R444	3	5	0.0 ± 0.0	15.2 ± 8.7	0.0 ± 0.0		1.7 ± 1.0	15.0 ± 8.6	0.0 ± 0.0	22.2 ± 15.6		14.3 ± 10.0
M. rileyi PHP1705	4 or indicated	5	0.0 ± 0.0 (n=2)	15.0 ± 7.1 (n=2)	2.8 ± 3.9 (n=2)		2.8 ± 3.3	18.1 ± 13.8	0.0 ± 0.0	11.2 ± 8.8		23.2 ± 11.9
Ecc15	2	2	2.5 ± 3.5	17.5 ± 3.5	10.0 ± 7.1		10.0 ± 7.1	15.3 ± 6.7	2.5 ± 3.5	6.3 ± 8.8		

Treatment			***Percent (%) males showing ewg***							
Pathogen	**n exp**	**dpi ewg taken**	***iso DrosDel***	***Df()/iso***	***iso ΔBaraA/iso***	***Df()/iso ΔBaraA***	***OR-R***	***Df()/OR***	***w; ΔBaraA/OR***	***Df()/w; ΔBaraA***
E. faecalis (OD5)	2	2	1.7 ± 2.9	17.4 ± 4.5	11.0 ± 9.2	12.5 ± 3.5	9.0 ± 1.3	22.0 ± 4.2	42.5 ± 38.9	42.5 ± 24.7

Supplementary information:

Identification of the BaraA C-terminus as IM22 from Uttenweiler-Joseph et al.

In 1998, Uttenweiler-Joseph et al. [4] described 24 immune-induced molecules by MALDI-TOF and informed predictions suggested that *BaraA* could encodes several of them [2]. We generated a knock out mutant for the *BaraA* gene (*BaraA*^{SW1}), which we validated by MALDI-TOF peptidomic analysis. Strikingly, we noticed an immune-induced peak at ~5981 Da in Linear mode collections that is absent in *ΔBaraA* flies (**Fig.** 2A); this mass closely resembled the 5984 Da estimated mass of IM22 from Uttenweiler-Joseph et al. [4], for which sequence was never determined. We took the Linear masses reported for then-unknown IMs from Uttenweiler-Joseph et al. [4] and post-hoc generated a standard curve with now-confirmed mass values from Levy et al. [2]. Our post-hoc standard curve corrects the mass of IM22 as found in Uttenweiler-Joseph et al. [4] to be 5973.5 Da. Using the same approach with our own linear data we find a mass of 5975.1 Da for our 5981 Da peak (**Supplementary data file 1**). With LCMS proteomics, we confirmed that the *BaraA* C-terminus is cleaved to remove 4 N-terminal residues, which should produce a putative 5974.5 Da peptide (**Fig** S2). Together these observations indicate the *BaraA* C-terminus encodes the following 53-residue mature peptide, matching the estimated mass of IM22: ARVQGENFVA RDDQAGIWDN NVSVWKRPDG RTVTIDRNGH TIVSGRGRPA QHY.

The *BaraA* gene is therefore involved in the production of over one third of the classical *Drosophila* IMs from Uttenweiler-Joseph et al. [4], including: IM5, 6, 8, 10, 12, 13, 20 (doubly-charged IM24 [2]), 22, and 24.

Sequence of the BaraA-Gal4 promoter construct

The following 1675bp sequence was cloned from the DrosDel isogenic background into the pBPGUw vector to drive a downstream Gal4 gene, and inserted into the VK33 attP docking site using BDSC line #24871:

Dif/dorsal binding site: **GGGHHNNDVH**

Rel binding site: GGRDNNHHBS

>iso_DrosDel_BaraA_promoter-Gal4

CTGCTACTCCTCTACACATTCGACTCCTTCGCCTTGCTGGCTGGGAAAAAATTTTGCATA
ATTTATGTGGGTGCCGCGCACACGGAGGTCCCGACGGATTCGAAGTATCCGAAGGATTCG
AAAGGAAAACAACGCACGAGCACCACGGCCAACTGATTTAAATGCAATTGCACTGAAGT
ATTTTGTTTGGCGAACGAAGCTGGATGAAATAGGGGGGTGTGGGGTTTTCTATTGAGAC
ATCTGCACGTGCAACCGGAAACATCCGAAGAGAACAGCACAGGCCGGGCTACGCCGGGCA
ATTTCTTTTCATTTGCCAAGGTGTTGAGTTGCACCAACATTCGACATCGACGTGGCCAGA
AGCCAACAAAAGCCAAGAGCCAAACCCCTTTTTGTGGTCACAAGTGTCGTCTATTTGTCG
TGGGCATCTTGGGCACCTTGGGCATCCTCGACATCCTTGCCATTTTGGTCTGGCCAAGAC
AAACAACCAGCAAATTTAGTGTATTTTGTGCATTTTTAAAATTGTCCAAATTTATGTGA
CACGCTGCGCCAATTGATCAGATTAAATAAACATGAGGCCAAGCGAATCGAATTTGGCT
TCACCAAGAAGACAATGCAGTCTGTATTCAAATGGGTGGGCGCATCCACCAAGCGGTGA
ATACAGTGACCGCTCGCTATAATGGACGGTCAGGTGTTACTTTAACTTAAAAAAATATG
TAACAAATCTTATCAAGTTTGAAATAGATTGAAATAGATTTGGTTATTGCATTCGAAAG
ATATATATTAAATTCGAATATTCCAAGAAATTTCATGAGAATGTCACTTATGTCATGAG
ATTATATTAACGTACGAATAAACAATGTATTTTCCAAAATTAAAAATAAAATTTAATTT
AATTACGCAGTACCTTTACACTATCAGTCGGAGGTAATAACTCATATAATTAGATTAGC
ATTAGATTTTAAAGCGAAAAACACTTAAAAGCTGAAATTATTAGACAACACTCTTAAAT
TAGTCGAGCTGATATATAGCCTCAAGTTTTGCTTAAATCCAAAGATAAAGGAATGCCTT
CAAAAATATATTTTGTTTTATACCAAGTGACAGCAGAGAATGGGGTTGCAATATCTTAA
AAGAGTTTCACTTAGCCAATATTTACTGCCATTGTTGGCCACCAAATAGTAGCAACCAGA
GACTTCCAGGAATATATTCTCGTGTCAAATGCAATCCACTTTAAATGCAACTATCTGGCG
GCTAAGAAAACCCGACAGTTTGATTCAAGTCGACGAAACAATATAAGCACGTGCTAAAT
AAAGAGACCTATGCAGTTAATACTCTTGTCATATTATAATATAATTTAGTGACATAAGT
TGCATGGTATACGAGTACTGAACAAGTTATGGCAGCTTTTCCAAATAAGCGATCACATA
TTCCGCGGGATGATGGGTGGATTTCTAGCATATGTGGATGCTTAATGGCTTATTGC**GGG**
TCAGGGCGGCGCAATCTGTTC**AGAAATTCCC**CGAACGCACACCCATTTCAGATCAGATTG
TGACGTTTT**GGGAAATTCT**TGACGATCGGTGTAAACAAGCTCAGCAACCAGATTCGATG
GCTATTTGCCGGCTATAAATACTAGAAACCATTCGATTGCACTCAGTTGAAGCTGGGCTC
TGGAACAGATCACA